

Magnetic Force Microscopy: Quantitative Results Treatment

2.7.1 MFM general concept

The magnetic force microscopy general concept is the registration of the force interaction between a magnetic probe and a sample's magnetic field. Today, there are two modes of the MFM operation: static MFM [1, 2] and dynamic MFM [3, 4].

In the **static MFM mode (dc)**, the interaction force F is measured through the detection of the cantilever deflection δ from the equilibrium position which is given by

$$\delta \approx \frac{F}{k} \quad (1)$$

where k – the cantilever spring constant (see [chapter 2.1.2 "Deflections under the vertical \(normal\) force component"](#)).

In the **dynamic MFM mode (ac)**, the change in resonant properties of the vibrating system cantilever-sample is registered. In this case the amplitude A , phase ϕ and resonant frequency ω_0 of the cantilever oscillation must be detected. If the force with the gradient $\partial F/\partial z$ acts on the cantilever in the vibration direction \mathbf{z} , the above mentioned parameters variation can be expressed as

$$\Delta\phi \approx \frac{Q}{k} \frac{\partial F}{\partial z} \quad (2)$$

$$\Delta A \approx \left(\frac{2A_0Q}{3\sqrt{3k}} \right) \frac{\partial F}{\partial z} \quad (3)$$

$$\Delta\omega_0 \approx -\frac{1}{2k} \frac{\partial F}{\partial z} \omega_0 \quad (4)$$

where k – cantilever spring constant, Q – vibrating system quality factor, A_0 – amplitude of cantilever oscillation at resonant frequency ω_0 in the absence

of external force gradient. As can be seen from (2)–(4), all three experimentally determined parameters are linear functions of the force derivative. In practice, however, $\partial F/\partial z$ is mainly determined by measuring the cantilever phase variation (2).

Let us estimate forces and their gradients which can be detected in the MFM. To do that, we calculate the interaction force between two point magnetic moments \mathbf{m}_1 and \mathbf{m}_2 separated by distance \mathbf{r} . Suppose one particle is on the cantilever tip and the other – on the sample surface. The field created by \mathbf{m}_1 at \mathbf{m}_2 location is:

$$H(\mathbf{r}) = \frac{3\mathbf{n}(n\mathbf{m}_1) - m_1}{r^3} \quad (5)$$

where \mathbf{n} – unit vector in the \mathbf{r} direction. The tip will experience the force which is defined as the energy gradient:

$$F = \nabla(m_2 H) \quad (6)$$

where \mathbf{B} – magnetic field from the sample. If \mathbf{m}_2 is independent of coordinates, expression (6) can be rewritten as:

$$F = (m_2 \nabla) H \quad (7)$$

Assuming that dipoles \mathbf{m}_1 and \mathbf{m}_2 are oriented along the Z -axis, the force of their interaction in accordance with (5), (7) is $F = -6m_1 m_2 / z^4$ and force gradient is $\partial F/\partial z = 24m_1 m_2 / z^5$. For iron (Fe) particles having diameter 100 Å magnetized to saturation ($m = 10^{-16}$ emu) and separated by distance 100 Å the resultant force is estimated as $\sim 10^{-11}$ N and force gradient is $\sim 10^{-2}$ N/m. According to expression (1), deflection of the silicon cantilever beam with spring constant $k = 0.1 \text{ N/m}$ ($k = 1/c$ is calculated using cantilever

dimension and Young's modulus, see (12) in [chapter 2.1.2 "Deflections under the vertical \(normal\) force component"](#)) under the point force $F = 10^{-11} N$ is equal to $\delta \approx 0.1 nm$. This value corresponds to the minimal detected deflection of modern AFM cantilevers.

The force gradient $\partial F/\partial z = 10^{-2} N/m$ results in the phase shift of the cantilever with quality factor $Q = 200$ and spring constant $k = 0.1 N/m$ equal to ϕ which is much more than the minimal detected signal.

Summary.

- Two modes of the tip-sample magnetic interaction exist: static MFM (dc) and dynamic MFM (ac).
- In the dc mode the interaction force is measured while in the ac mode - the force gradient.
- Dynamic mode of MFM operation is more sensitive to the magnetic field variation than the static one.
- In both modes the detected signals do not depend directly on the sample magnetic properties. Therefore, it is necessary to consider available algorithms of the quantitative interpretation of MFM data (see [2.7.2 Algorithms for the physical parameters of the sample obtaining](#)).

References

1. Appl. Phys. Lett. 50, 1455 (1987).
2. J. Appl. Phys. 62, 4293 (1987).
3. P. Grutter, H.J. Mamin, D. Rugar, in Scanning Tunneling Microscopy II, edited by R. Wiesendanger and H.-J. Guntherodt (Springer, Berlin, 1992) pp. 151-207.
4. S. Manalis, K. Babcock, J. Massie, V. Elings, M. Dugas, Appl. Phys. Lett. 66, 2585 (1995).

2.7.2 Algorithms for the physical parameters of the sample obtaining

What information about the sample magnetic properties can we reveal knowing the derivative of the magnetic interaction force with respect to vertical direction $\partial F/\partial z$?

a. Spatial periodicity and domain structure dimensions. Qualitative analysis

To get the sample qualitative picture and observe its magnetic properties (for example, spatial periodic domain structure), there often is enough to know the derivative of magnetic interaction force. It is clear that the detected force of magnetic interaction and field are actually constant as tip moves over domain. When the cantilever passes across a domain wall, a smoothed step of the resonance oscillation phase and amplitude is observed which corresponds to the force change. This is, in fact, the only picture we can obtain for the sample with a rather coarse magnetic structure.

b. Quantitative analysis (classical approach)

To quantify the experimental data, the chart shown in **Fig. 1** is normally employed.

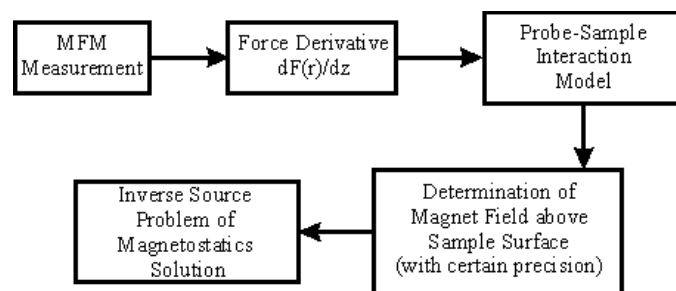


Fig. 1. MFM results processing chart

First, the $\partial F/\partial z$ value is calculated in accordance with expressions (2)–(4) of [2.7.1 MFM general concept](#) using experimental results. Next, the magnetic field is rendered in the tip vicinity. To do that we need to choose a physical model that describes the magnetic probe interaction with external magnetic field. Depending on the probe used, these models can be classified as follows [1]:

- Hard magnetic cantilever.
 - General expression of the interaction force between a magnetic cantilever and a sample (see [2.7.3 Interaction of the hard magnetic cantilever with the magnetic field of the studied sample \(general case\)](#)).
 - Point dipole approximation (see [2.7.4 Dipole effective magnetic moment approximation](#)).
 - Point monopole approximation (see [2.7.5 Effective monopole magnetic charge approximation](#)).
- Soft magnetic cantilever.
- Paramagnetic cantilever

Thus, having chosen one of the mentioned models, one can render the magnetic field distribution in space above a sample. Notice that regardless of the model chosen, the magnetic field map will be rendered to some accuracy because firstly, the probe oscillation amplitude is considered theoretically to be infinite small as compared to probe-sample separation. In practice, this condition is almost never satisfied so the amplitude finiteness must be taken into consideration. In other words, in MFM, $\partial F/\partial z$ is measured not locally but in some tip vicinity dependent on its oscillation amplitude. Experimental magnitude of $\partial F/\partial z$ is in fact the averaged value in this vicinity. Secondly, the finiteness of the tip-sample interaction region is to be taken into consideration, too.

The last step of the chart (Fig.1) is the sample magnetic structure representation. To determine the studied surface magnetization (distribution of unit volume magnetic moment), the so called inverse source problem of magnetostatics should be solved. Remember that the forward problem is the field calculation from the known sources while the inverse problem is the sources positions determination basing on the information about the field structure. Thus, the inverse problem solution means determination of magnetization distribution across the sample surface under given magnetic field distribution in space. Because the field distribution has been previously rendered to some accuracy, the magnetization distribution will be rendered with a gross error. Moreover, in some cases the inverse problem can not be solved in principle. That's why another algorithm of MFM data quantitative interpretation is needed.

c. Parametric method (alternative to classical approach)

To interpret quantitatively the experimental results, the following algorithm shown in Fig. 2 is proposed.

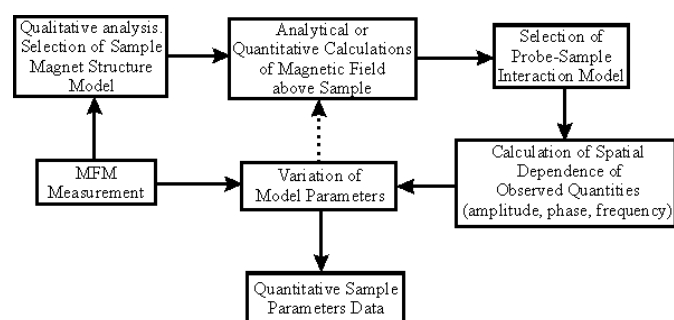


Fig. 2. Algorithmic diagram of MFM data analysis

First, the qualitative analysis of the studied sample is performed. Then, the acquired qualitative relations are compared to theoretical ones obtained from model problems. Here it means that we can choose between various theoretical expressions for the derivative of the magnetic field force acting on the tip calculated for the most common magnetic structures. In particular, such database should contain as a minimum qualitative MFM results for the following magnetic structures: single magnetic bubble, periodic magnetic bubble pattern (with variation in size and magnetization orientation), 2.7.11 Magnetic field of cylinder domains; single laminar domain, periodic pattern of laminar domains (with variation in size and magnetization orientation); periodic pattern of parallel domains, 2.7.12 Magnetic field of periodic parallel domains, etc. Having compared experimental data with an image from the database, we can choose the sample configuration model that fits best.

Further, we select a model of the tip interaction with an external magnetic field (these models are mentioned above) and within the framework of this model compute variation in detected parameters (phase, amplitude, frequency) having set previously the problem initial parameters: probe geometry, probe magnetization, tip-sample separation. Then, by varying the model unknown parameters depicting the sample magnetic structure, achieve the best agreement between calculation and measurement. These unknown parameters that provide the agreement represent the quantitative data about the sample magnetic structure. Sometimes, limited experimental data restrict the determination of the model parameters uniquely with high accuracy. In this case, according to the analysis results it is possible to limit the range of allowable values of the model parameters.

Thus, to quantify the magnetic characteristics of the studied structures within the framework of this algorithm, it is necessary:

- to perform the qualitative MFM investigation of the sample structure.
- to choose the model of the magnetic field distribution in the sample.
- to choose the model of the probe interaction with the sample magnetic field.
- to adjust such unknown parameters of the sample magnetic field model that calculation and measurement agree well.

where r_s – distance from the point of origin to the sample magnetic domain $M_s(r)$ and n_s – normal vector to the sample surface. Substituting into equations (1), (2) instead of $H(r)$ expressions (5) and (6), we can find F and F_n' .

■ Summary

- Described is a model that in a general case allows to calculate the force acting on the probe with known magnetic characteristics at a given point in space over the sample having arbitrary distribution of the magnetization vector and its derivative.
- This model is valid only for hard magnetic cantilevers and samples when mutual interference of sample $M_s(r)$ and probe $M_T(r)$ magnetization is not taken into consideration.

■ References

1. P. Grutter, H.J. Mamin, D. Rugar, in Scanning Tunneling Microscopy II, edited by R. Wiesendanger and H.-J. Guntherodt (Springer, Berlin, 1992) pp. 151-207.
2. L.D. Landau, E.M. Lifshitz. Theoretical Physics, vol. 2, Field Theory, Nauka, 1973, 504 p. (in Russian).
3. W.F. Brown. Magnetostatic Principles in Ferromagnetism (Amsterdam 1962).
4. U. Hartmann. J. Appl. Phys. 64, 1561 (1988).

2.7.4 Dipole effective magnetic moment approximation

Within the framework of the point dipole model the probe magnetic properties are considered to be entirely defined by its dipole effective magnetic moment m_{eff} as well as by position r_m of this resultant moment inside the cantilever (Fig. 1).

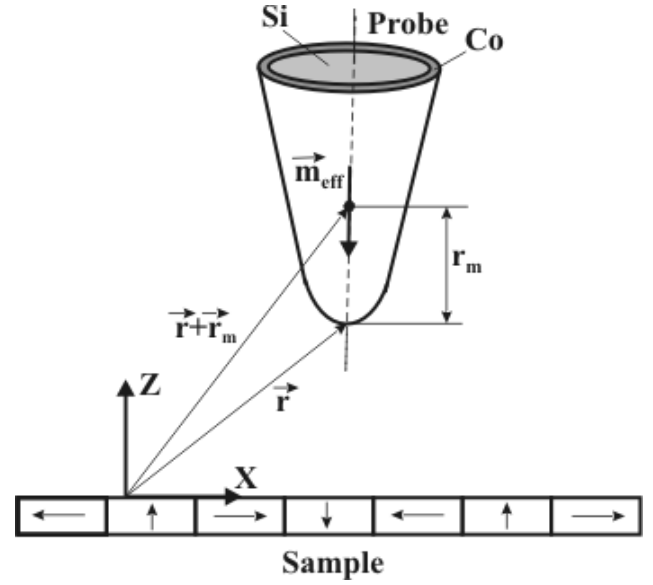


Fig. 1. Dipole model of point interaction between probe and magnetic field

If the probe tip is perpendicular to the sample surface (n and Z are collinear, see Fig. 1), then expressions (3), (4) of 2.7.3 Interaction of the hard magnetic cantilever with the magnetic field of the studied sample (general case) in the point dipole approximation can be rewritten as:

$$F(r) = m_{eff} \cdot \frac{\partial H(r + r_m)}{\partial z} \quad (1)$$

$$\frac{\partial F(r)}{\partial z} = m_{eff} \cdot \frac{\partial^2 H(r + r_m)}{\partial z^2} \quad (2)$$

that is both F and $\partial F/\partial z$ depend on the field magnitude only at conditional point $r + r_m$ where dipole is placed.

To determine field magnitudes that make point dipole model applicable, one should compare equations (1) of this section and (3) of 2.7.3 Interaction of the hard magnetic cantilever with the magnetic field of the studied sample (general case) written for the same field. Applicability criteria to within second derivatives is given by (simplified formula from [1]):

$$\frac{l^2}{H_i} \nabla H_i \ll 1 \quad (3)$$

where H_i – field components ($i = x, y, z$), Δ – Laplacian, l – characteristic tip size (linear

dimension of tip area interacting with magnetic field). This expression can be simplified as

$$\frac{l^2}{\zeta^2} \ll 1 \quad (4)$$

where ζ – characteristic scale of field variation, i.e. the distance at which the field changes are of its own order.

Model parameters m_{eff} and r_m are determined experimentally for every cantilever. A calibration is performed in the known magnetic field. For this purpose, microscopic loops with flowing current and calculated magnetic field distribution [2] can be used. They are fabricated photolithographically on the sample surface. The force derivative $\partial F/\partial z$ is measured at different heights above the sample surface. Then parameters m_{eff} and r_m are varied to get the best agreement between measured $\{\partial F(r)/\partial z\}_i$ and calculated $\{m_{eff} \partial^2 H(r+r_m)/\partial z\}_i$ values.

Despite the simplicity of this method of the cantilever calibration and further interpretation of MFM results, this model is applicable only to some cantilever types and magnetic samples. It was shown, that for samples with sufficiently different attenuation length of magnetic field but having the same field magnitude as that of the calibrating sample, values of m_{eff} and r_m must be quite different. In [2] the dependence of m_{eff} and r_m on attenuation length was studied using the calibrating Ω -shaped metallic loops at constant cantilever oscillation parameters. It is well known that the magnetic field on the axis of the ring with flowing direct current is inversely proportional to the ring radius and attenuation length is about the radius R . Table 1 presents dependences of m_{eff} and r_m on radius of studied rings [2].

m_{eff}, A^2	R, m	r_m, m	l, m
$6,009 \cdot 10^{-15}$	$6,030 \cdot 10^{-7}$	$5,2 \cdot 10^{-7}$	$9,285 \cdot 10^{-7}$
$4,744 \cdot 10^{-14}$	$1,419 \cdot 10^{-6}$	$1,31 \cdot 10^{-6}$	$2,564 \cdot 10^{-6}$
$2,042 \cdot 10^{-13}$	$2,369 \cdot 10^{-6}$	$2,86 \cdot 10^{-6}$	$5,292 \cdot 10^{-6}$

Table 1. Values of m_{eff} , r_m and l at various R

In table 1 parameter l stands for the tip length counted off from its end and contributing to the interaction with the magnetic field. In [2] it is determined as follows. First, the tip magnetization is measured using superconducting quantum magnetometer and magnetic moment per tip coating unit volume is calculated. Then, considering the tip as a regular quadrangular pyramid, integration is performed to determine the sum magnetic moment. The region of integration l is varied to fit the experimental value of m_{eff} . From table 1 it follows that l is a linear function of the ring radius R and hence is proportional to attenuation length ζ .

In that way, since effective magnetic dipole depends on sample magnetic characteristics, it is problematic to quantify MFM data for classical silicon tips with magnetic coating. Nevertheless, this model is useful for qualitative interpretation of measurement results or for quantifying data obtained with tips made of magnetic nanoparticles.

Summary

- In the dipole effective magnetic moment model it is considered that tip magnetic properties are entirely defined by its effective magnetic dipole moment m_{eff} and position r_m of this resultant moment inside the cantilever.
- This model is applicable for qualitative analysis of MFM data in case of meeting the conditions (3), (4).
- Quantitative analysis of MFM results is difficult because parameters of effective magnetic dipole themselves are dependent on the studied sample magnetic characteristics.

References

1. U. Hartmann, J. Physcs Letters A. 137, 475 (1989).
2. J. Lohau, S. Kirsch, A. Carl et al, J. Appl. Phys. 86, 3410 (1999).
3. P. Grutter, H.J. Mamin, D. Rugar, in Scanning Tunneling Microscopy II, edited by R. Wiesendanger and H.-J. Guntherodt (Springer, Berlin, 1992) pp. 151-207.

2.7.5 Effective monopole magnetic charge approximation

Along with the model of point dipole (see chapter 2.7.4 Dipole effective magnetic moment approximation), an alternative model of point monopole charge exists which allows to describe in some cases the cantilever interaction with the magnetic field.

Consider the cylinder of length L and radius R uniformly magnetized along lateral surface in the z -axis direction as a magnetic probe (Fig. 1). Magnetic material in Fig.1 is cobalt.

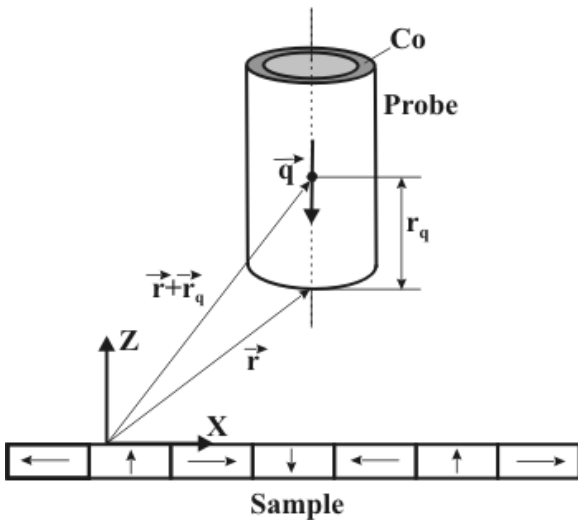


Fig. 1. On the monopole approximation

Let the bottom end of the probe be at the point with radius-vector r . Denote z as the unit vector along the z -axis. Suppose that the attenuation length of magnetic field ζ is much less than L , then the magnetic field at the probe top end $H_z(r + zL) \rightarrow 0$. Moreover, let magnetic field vector H be almost independent on x and y at least within the distance of probe radius R . Then the force acting on the probe along z -axis in accordance with chapter 2.7.3 Interaction of the hard magnetic cantilever with the magnetic field of the studied sample (general case) is given by:

$$F_z(r) = \frac{m}{L} \int_0^L \frac{\partial H_z(r + Zz)}{\partial z} dz = \frac{m}{L} (H(r + zL) - H(r)) = -\frac{m}{L} H_z(r) \quad (1)$$

where m – total magnetic moment of the cylinder. If the probe is of finite length, i.e. condition $\zeta \ll L$ is not met properly or probe section is not constant, the calculation and measurement agree well in case

the point monopole is supposed to be placed some distance r_q from the probe end.

$$F_z(r) = qH_z(r + r_q) \quad (2)$$

where $q = -m/L$ – magnetic moment per cylinder unit length which is called the monopole charge.

In the point monopole model it is considered that the probe magnetic properties are completely defined by its effective magnetic monopole charge q and by position r_q of this resultant monopole inside the probe (Fig. 1). In this case, the force acting on the probe in the z -axis direction is proportional to the magnetic field magnitude and is given by (2) while its derivative is

$$\frac{\partial F_z(r)}{\partial z} = q \frac{\partial H_z(r + r_q)}{\partial z} \quad (3)$$

As can be seen from (2), the effective force just reflects the magnetic force distribution and force directional derivative – the field derivative correspondingly.

In practice, this model is used by analogy with the dipole model described in chapter 2.7.4 Dipole effective magnetic moment approximation. Using calibrating samples with known magnetic field distribution, q and r_q parameters are varied to obtain the best agreement between theory and experiment. This model works well at large distances from the sample surface when the field changes slowly. However, like in case of dipole approximation, magnitudes of q and r_q must be different for samples with the field attenuation length different from that of the calibrating sample.

■ Summary

- In the model of effective monopole magnetic charge it is considered that the probe magnetic properties are completely defined by its effective magnetic monopole charge q and by position r_q of this resultant monopole inside the probe.
- It is difficult to quantify MFM data in the framework of this model because parameters of effective magnetic monopole are themselves dependent on the studied sample's magnetic characteristics.

- This model can be applied to analysis of MFM data only in case of narrow tips with constant section at distances exceeding much the magnetic field attenuation length.

References

1. U. Hartmann, J. Physcs Letters A. 137, 475 (1989).
2. J. Lohau, S. Kirsch, A. Carl et al, J. Appl. Phys. 86, 3410 (1999).
3. P. Grutter, H.J. Mamin, D. Rugar, in Scanning Tunneling Microscopy II, edited by R. Wiesendanger and H.-J. Guntherodt (Springer, Berlin, 1992) pp. 151-207.

2.7.6 Interaction between soft magnetic probe and magnet sample

In chapter 2.7.3 Interaction of the hard magnetic cantilever with the magnetic field of the studied sample (general case) we described the general model of a hard magnetic probe interaction with a magnetic field of a sample and neglected the fact that a tip and a sample can mutually affect their magnetic characteristics. This influence should, in fact, be taken into account when constructing theoretical models of a hard magnetic tip interaction with the sample magnetic field. An assumption that the sample magnetization is not affected by the tip magnetic field is a good approximation for hard magnetic samples and is not valid for the soft ones, for example, for *NiFe* (permalloy) [1, 2, 3].

In [4] it is shown that the tip magnetic field affects the magnetic properties of the sample and vice-versa in case when magnetic field of one exceeds the magnetic anisotropy field of the other:

$$H^T > H_K^S \text{ or } H^S > H_K^T \quad (1)$$

where H^T and H^S – magnetic fields of tip and sample and, respectively, H_K^T , H_K^S – magnetic anisotropy fields. Near the tip and sample surface the magnetic field can be taken equal to $4\pi M$, where M – a material magnetization, and can exceed much the magnetic anisotropy field of a soft magnetic material like iron or permalloy. To avoid this effect it is necessary to increase the tip-sample separation [5] that results in sufficient lateral resolution deterioration.

In [2, 3] the theories were developed that take into account the magnetization vector rotation under the external magnetic field. These theories predict the appearance of an additional attraction force between a tip and a sample because magnetic moments in a sample tend to align with the tip magnetic field and vice-versa. This effect was observed in permalloy [5].

Perhaps, the most successful way of the tip-sample interaction description is the determination of a system minimum energy. The method is a sample decomposition into infinitesimal cells and a subsequent calculation of the minimum energy of magnetic states taking into consideration the exchange interaction, anisotropy energy and magnetostatics. In [6] this method was used for the calculation of the permalloy domain walls distribution in the presence of the iron tip. In [7] the energies of the tip magnetic states equilibrium and the resultant force acting on it in the magnetic field was calculated by integration of the Landau-Lifshits-Hilbert equation.

Summary

- In case when magnetic field of a sample exceeds the magnetic anisotropy field of a tip and vice-versa, they can mutually affect the magnetic characteristics of each other.
- Presented is a brief review of quantification methods of a soft magnetic tip interaction with a sample magnetic field and, accordingly, a soft magnetic sample interaction with a tip magnetic field.

References

1. T. Goodenhenrich, U. Hartmann, M. Anders, C. Heiden: J. Microscopy 152, 527 (1988).
2. J.J. Saenz, N. Garcia, J.C. Slonczewski; Appl. Phys. Lett. 53, 1449 (1988).
3. D.W. Abraham, F.A. McDonald: Appl. Phys. Lett. 56, 1181 (1990).
4. U. Hartmann: J. Appl. Phys. 64, 1561 (1988).
5. H.J. Mamin, D. Rugar, J.E. Stern, R.E. Fontana, Jr., P. Kasiraj: Appl. Phys. Lett. 55 318 (1989).
6. M.R. Scheinfein et al. J. Appl. Phys. 67, 5932 (1990).
7. M. Mansuripur: IEEE Trans. Magn. 25, 3467 (1989).

2.7.7 Interaction between paramagnetic probe and magnet sample

If magnetic field $H(r)$ produced by a sample is known, then force F on a magnetic cantilever and its derivative F'_n in direction n can be calculated integrating the force acting on the elementary volume dV over the whole ferromagnetic film volume V_c [1]:

$$F = \int_{V_c} \nabla_r (M_T(r_V) \cdot H(r + r_V)) dV \quad (1)$$

$$F'_n = \int_{V_c} n \cdot \nabla_r (n \cdot \nabla_r (M_T(r_V) \cdot H(r + r_V))) dV \quad (2)$$

where $M_T(r_V)$ – magnetic moment of the unit volume of the cantilever magnetic coating, $H(r + r_V)$ – magnetic field from the sample, r – vector corresponding to the probe's tip position, r_V – vector corresponding to the elementary magnetic moment position relative to r , n – normal vector to the probe surface collinear with its principal axis of symmetry (Fig. 1).

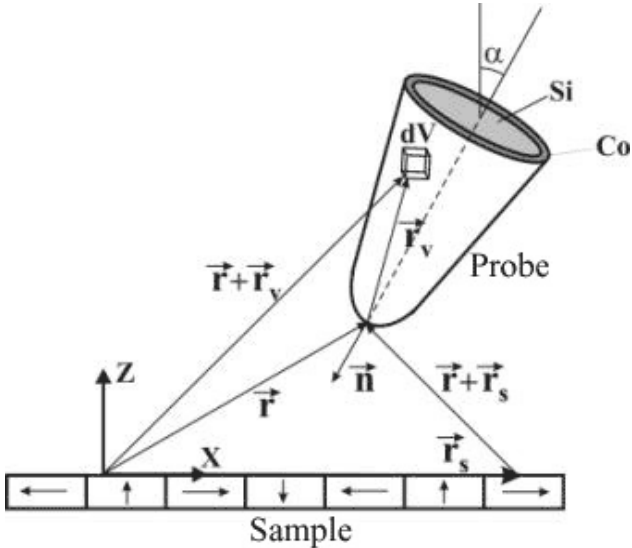


Fig. 1. The model geometry used to calculate the force and its derivative acting on a tip

If vector n is directed along the Z -axis, then force (1) and its Z -derivative (2) can be written as

$$F = \int_{V_c} \left(M_{Tx} \frac{\partial H_x}{\partial z} + M_{Ty} \frac{\partial H_y}{\partial z} + M_{Tz} \frac{\partial H_z}{\partial z} \right) dV \quad (3)$$

$$F' = \frac{\partial F}{\partial z} = \int_{V_c} \left(M_{Tx} \frac{\partial^2 H_x}{\partial z^2} + M_{Ty} \frac{\partial^2 H_y}{\partial z^2} + M_{Tz} \frac{\partial^2 H_z}{\partial z^2} \right) dV \quad (4)$$

For paramagnetic materials, the magnetization vector M_T depends on external magnetic field magnitude [2]. Particularly, if external magnetic field is zero, the magnetization inside the material is zero. Otherwise, it is equal to [2]

$$M_{Ti} = \chi_{ik} H_k^* \quad (5)$$

where χ_{ik} – tensor of material magnetizability, H_k^* – magnetic field inside the material induced by external field H . The relation between vectors H and H^* can be obtained from boundary conditions for normal (denoted as n) and tangential (denoted as t) components of vectors H , $B_i = \mu_{ik} H_k$ at two media interface [2]

$$H_t = H_t^*, \quad B_n = B_n^* \quad (6)$$

where $\mu_{ik} = 1 + 4\pi\chi_{ik}$ – tensor of the medium magnetic permeability. Thus, the magnetization vector of the paramagnetic probe M_T depends on external magnetic field spatial distribution in accordance with formulas (5,6).

As an MFM tip, a carbon nanotube deposited onto the standard cantilever tip, can be used [3, 4]. Carbon is a paramagnetic material, therefore, the tip magnetization is a function of external magnetic field in accordance with (5). Let us determine the magnetization of the nanotube placed in a uniform magnetic field.

The carbon nanotube is cylindrically shaped and its length is normally much more than the radius. In this case, its geometry can be approximated by an ellipsoid of revolution. The relationship between magnetization of the ellipsoid and uniform external magnetic field H is given by [5]

$$H_i^* + n_{ij} (\mu_{jk} H_k^* - H_j^*) = H_i \quad (7)$$

where n_{ij} – tensor of demagnetizing factors. Then, determining H^* from (7) and substituting it into (5), we can obtain the magnetization of the nanotube in the uniform magnetic field.

Summary

- Described is a model which allows to determine in a general case the force and its derivative acting on a paramagnetic tip with known magnetic characteristics.
- The magnetization vector of paramagnetic tip depends on spatial distribution of external magnetic field in accordance with formulas (5,6).
- Magnetization of a nanotube in a uniform magnetic field is considered.

References

1. P. Grutter, H.J. Mamin, D. Rugar, in Scanning Tunneling Microscopy II, edited by R. Wiesendanger and H.-J. Guntherodt (Springer, Berlin, 1992) pp. 151-207.
2. Ch. Kittel. - "Introduction into the solid state physics", Moscow: "Nauka", 1978, 792 pp. (in Russian).
3. Akita S., Nakayama Y., Arie T. Yoshida N.: J. Appl. Phys. 34, 43-45 (2001).
4. Akita S., Nakayama Y., Arie T. Nishijima Hidehiro.: J. of Vacuum Science and Technology B 18, 1 (2000) 104-107.
5. L.D. Landau, E.M. Lifshits - "Theoretical physics volume 8. Electrodynamics of continuum", Moscow: "Nauka", 1982, 620 pp. (in Russian).

2.7.8 Methods of magnet probe parameters estimation

At the present time there are a lot of MFM probes of various types [1]. The proper choice of a probe for studying a specific microstructure is sometimes an independent and complicated problem and is determined by a researcher experience. To simplify the problem, one needs to have techniques that allow to quantify magnetic characteristics of probes, the major of which are the magnetic moment per unit volume of a film (magnetization) and magnetic coating coercivity.

To characterize probes, many methods were proposed from analysis of their interaction with a hard disk or magnetic tape surface [2], including measurements of magnetic heads field [3] to even exotic technique connected with studying the

magnetotactical bacteria [4]. However, the simplest from the standpoint of interpretation is the technique of the interaction detection between the tip and the magnetic field of a current-carrying microconductor. The magnetic field of such systems can be calculated with a high accuracy using methods of conventional magnetostatics even in an analytic form in most cases.

In [5] it was proposed to use a straight current carrying strip line for this purpose. The scanning was performed across the strip in the presence of external magnetic field. Determined was the coercitive field (along and across the tip) for the following coatings *NiFe*, *CoCr* (150A, 400A), *CoCrPt*, *Co*. Also, the authors of [5] succeeded in estimating an effective magnetic moment. However, in [6] the role of the electrostatic interaction with a conductor was revealed and a method of electrostatic and magnetic interaction separation was proposed. Though in [5] the electrostatic interaction was not taken into account, the sample was prepared very thoroughly. In particular, a thin layer of gold several tens of angstrom thick was deposited over a dielectric layer. The golden coating was connected to the ground potential that apparently minimized the electrostatic interaction of a probe with a current-carrying conductor.

Further development of magnetic probe calibration techniques led to the use of a current Ω – ring magnetic field. In [7] the rings of diameter 1-5 micron and strip width of 200 nm manufactured by submicron lithography were first used for the magnetic tip calibration. However, the qualitative analysis of the experiment was not quite correct, in particular because the authors used the model of a point dipole assuming that it was situated precisely at the tip end. As is shown in [8], such assumption results, after accurate data processing, in unreasonable magnitudes of effective monopole and dipole. A more accurate experiment [8] permitted to determine the magnitude of magnetic dipole and its location inside the sample. It was shown experimentally that the effective dipole should be located approximately in the center of an area whose vertical dimension depends on characteristic attenuation length of magnetic field. This length is proportional to the ring radius. In this case, the cantilever magnetic moment becomes dependent on the radius of the ring used in experiment. A theoretical calculation by integration over the

interaction region under the assumption that the magnetic moment of the film unit volume is equal to macroscopic saturation magnetization of the coating material, gives a reasonable agreement with measurement results.

Thus, the effective moment of the tip with magnetic coating depends on what kind of magnetic structure is studied. Therefore, for such tips it is reasonable to measure and tabulate not the magnetic moment of the tip but the magnetic moment per unit area of a coating film. On the other hand, determination of the total magnetic moment for tips with localized magnetic moment [9, 10, 11, 12] is quite reasonable and in this case its location is determined unambiguously.

To measure the hysteresis loop of tips magnetic coatings, in [13] it is proposed to place the whole cantilever in a magnetic field with changing gradient (external coil produces field of 0.2 Oe) and frequency close to the cantilever resonant frequency. Measuring the amplitude of oscillations, the force magnitude was estimated and the magnetic moment was determined in relative units. Varying the external field by permanent magnet (up to 280 Oe), the authors measured the hysteresis loop for such coatings as $CoCrPt/NiFe$, $Co_{80}Pt_{20}$, $CoCr$.

In chapter 2.7.4 Dipole effective magnetic moment approximation and chapter 2.7.5 Effective monopole magnetic charge approximation the technique of determination of point dipole and monopole effective value is described in detail. However, as it is pointed out before, the quantitative characteristic of point dipole (monopole) and its location in a probe depend much on the attenuation length of a studied sample magnetic field. Therefore, in order to unambiguously calibrate the magnetic probe it is necessary to measure the magnetization of the probe ferromagnetic hard magnetic material.

For this purpose, a special [Flash model](#) was developed which calculates theoretically the change in amplitude, phase and frequency of a probe oscillation or the static deflection of a probe during the second pass across a sample surface in the standard AC MFM mode. In this model the current-carrying rectangular conductor acts as the sample for study. The spatial distribution of magnetic field

produced by the current in a rectangular strip is obtained in chapters 2.7.9 Magnetic field of rectangular conductor with current.

Utilizing a general case of the model of a hard magnetic probe interaction with a sample magnetic field (see chapter 2.7.3 Interaction of the hard magnetic cantilever with the magnetic field of the studied sample (general case)), a theoretical analysis of the current-carrying strip magnetic field interaction with probes of various types: cylindrical, spherical, conical, and diamagnetic conical with ferromagnetic coating is performed (see chapter 2.7.9 Magnetic field of rectangular conductor with current and [Appendices](#) for it). The models allow to study the effect of variation of sample geometry, probe parameters (dimensions, magnetization, stiffness, resonant frequency, quality factor), measurement mode parameters within permissible limits. The calculation of the amplitude, phase and frequency change is performed in accordance with formulas (18), (16), (11) of [chapter 2.3.4 "Cantilever small oscillations in a force field"](#).

Thus, substituting the experimental data of the strip line magnetic field MFM measurements in AC mode into this Flash model, it is possible to compare them with theoretical ones at various probe and sample parameters. Hence, using this model, one can determine unknown parameters of the probe (magnetization, in particular) by varying model parameters until experimental and theoretical data fit well. Moreover, a set of optimal parameters can be selected that provides the maximum change of detected signals from given samples.

■ Summary

- A review of magnetic probes calibration methods and accompanying problems is presented.
- The most widespread and simple enough technique of a probe magnetic characteristics determination is its calibration in the magnetic field of a current-carrying microconductor.
- Presented are the theoretical aspects of a Flash model which allow to calculate the measured in a standard AC MFM mode parameters depending on the sample parameters (strip line/ Ω -ring).

- By means of the developed Flash model one can determine unknown probe parameters appearing in an experiment and choose an optimal set of a system theoretical parameters that provides the maximum change in detected signals.

■ References

1. P. Grutter, H.J. Mamin, D. Rugar, in Scanning Tunneling Microscopy II, edited by R. Wiesendanger and H.-J. Guntherodt (Springer, Berlin, 1992) pp. 151-207.
2. D. Rugar, H.J. Mamin, P. Guethner et al, J. Appl. Phys. 68, 1169 (1990).
3. S. Khizroev, W. Jayasekara, J. Bain et al, IEEE Trans. Magn. 34, 2030 (1998).
4. R.B. Proksch, T.E. Shaffer, B.M. Moskowitz, Appl. Phys. Lett. 66, 2582 (1995).
5. K.L. Babcock, V.B. Elings, J. Shi et al, Appl. Phys. Lett. 69, 705 (1996).
6. T. Alvarez, S.V. Kalinin, D.A. Bonnell, Appl. Phys. Lett. 78, 1005 (2001).
7. L. Kong, S.Y. Chou, Appl. Phys. Lett. 70, 2043 (1997).
8. J. Lohau, S. Kirsch, A. Carl et al, J. Appl. Phys. 86, 3410 (1999).
9. M.R. Koblischka, U. Hartmann, T. Sulzbach, Thin Solid Films 428, 93 (2003).
10. T. Arie, H. Nishijima, S. Akita et al, J. Vac. Sci. Technol. B 18, 104 (2000).
11. T. Arie, N. Yoshida, S. Akita et al, J. Phys. D 34, L34 (2001).
12. N. Yoshida, T. Arie, S. Akita, Y. Nakayama, Physica B: Cond. Matt. 323, 149 (2002).
13. J. Lohau, S. Kirsch, A. Carl et al, J. Appl. Phys. 86, 3410 (1999).

2.7.9 Magnetic field of rectangular conductor with current

Flash model

Let us calculate the spatial distribution of magnetic field generated by density j current passing through a rectangular conductor having length L , width w and thickness h , $L \gg h$ and $L \gg w$ (Fig. 1).

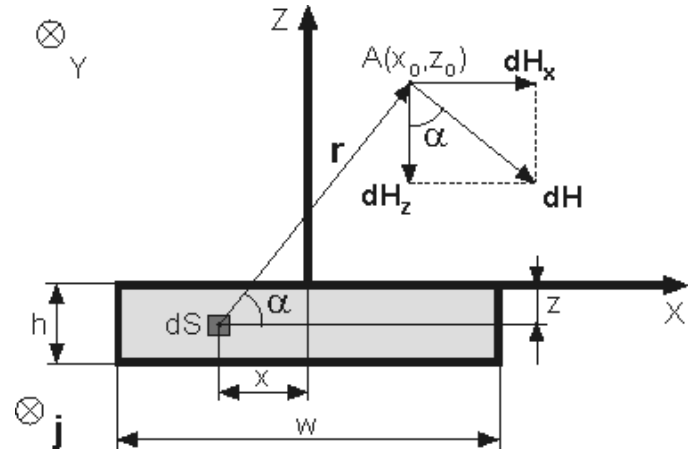


Fig. 1. Cross-section of rectangular conductor

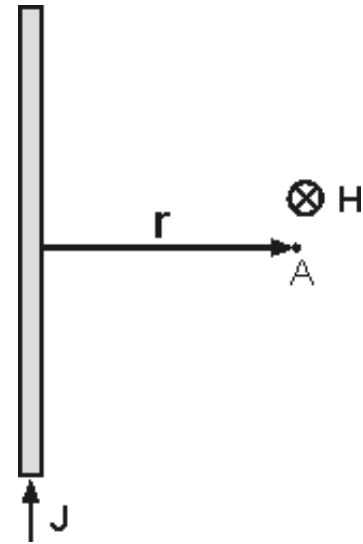


Fig. 2. Schematics of infinitely-thin wire which carries constant current J

According to the Biot-Savart-Laplace law [1, 2], magnetic field H from the infinitely-long thin current-carrying wire at distance r (Fig. 2) in Gaussian coordinates is given by

$$H = \frac{\beta J}{r} \tag{1}$$

where $\beta = \frac{2}{c}$, c – light velocity, J – current in the wire, the magnetic field vector and vector product $J \times r$ being codirectional.

Dividing the conductor cross-section into a infinite number of wires having section $dS = dx dz$ as in Fig. 1, we can write the magnetic field of elementary wire at point $A(x_0, y_0)$ in accordance with formula (1) as follows:

$$\begin{aligned} dH_x(x_0, z_0) &= \frac{\gamma \sin \alpha}{r} dx dz \\ dH_y(x_0, z_0) &= 0 \\ dH_z(x_0, z_0) &= \frac{-\gamma \cos \alpha}{r} dx dz \end{aligned} \quad (2)$$

where $\gamma = \beta j$, j – current density, $r = \sqrt{(x_0 - x)^2 + (z_0 + z)^2}$ – smallest distance from elementary wire to point A, α – angle between vector r and axis X, and

$$\begin{aligned} \sin \alpha &= \frac{z_0 + z}{\sqrt{(x_0 - x)^2 + (z_0 + z)^2}}, \\ \cos \alpha &= \frac{x_0 - x}{\sqrt{(x_0 - x)^2 + (z_0 + z)^2}}. \end{aligned} \quad \text{We will not}$$

calculate further the magnetic field along the Y-axis because at an arbitrary point (x_0, y_0, z_0) it obviously is zero.

The total magnetic field at point $A(x_0, y_0)$ can be calculated by integration of expression (2) over the conductor cross-section:

$$\begin{aligned} H_x(x_0, z_0) &= y \int_{-w/2}^h \int_{-w/2}^h dH_x(x_0, z_0) dx dz = y \left[\int_{-w/2}^{x_0} \frac{z_0 + z}{(x_0 - x)^2 + (z_0 + z)^2} dx + \int_{x_0}^{w/2} \frac{z_0 + z}{(x_0 - x)^2 + (z_0 + z)^2} dx \right] dz = \\ &= y \left[\int_0^{w/2+x_0} \frac{z_0 + z}{p^2 + (z_0 + z)^2} dp - \int_0^{x_0-w/2} \frac{z_0 + z}{p^2 + (z_0 + z)^2} dp \right] dz \\ H_z(x_0, z_0) &= y \int_{-w/2}^h \int_{-w/2}^h dH_z(x_0, z_0) dx dz = y \left[\int_{-w/2}^{x_0} \frac{x - x_0}{(x_0 - x)^2 + (z_0 + z)^2} dx + \int_{x_0}^{w/2} \frac{x - x_0}{(x_0 - x)^2 + (z_0 + z)^2} dx \right] dz = \\ &= y \left[\int_0^{w/2+x_0} \frac{-p}{p^2 + (z_0 + z)^2} dp + \int_0^{x_0-w/2} \frac{p}{p^2 + (z_0 + z)^2} dp \right] dz \end{aligned} \quad (3)$$

where we made the transformation of variable: $p = x_0 - x$. Integrals of the following type

$$\begin{aligned} \tilde{H}_x(p_0, z_0) &= y \int_0^h \int_0^{p_0} \frac{z_0 + z}{p^2 + (z_0 + z)^2} dp dz, \\ \tilde{H}_z(p_0, z_0) &= y \int_0^h \int_0^{p_0} \frac{-p}{p^2 + (z_0 + z)^2} dp dz \end{aligned} \quad (4)$$

can be expressed through analytical functions as follows:

$$\begin{aligned} \tilde{H}_x(p_0, z_0) &= \frac{y}{2} \left[p_0 \ln \left(1 + \frac{h^2 + 2z_0 h}{p_0^2 + z_0^2} \right) + 2(z_0 + h) \arctan \left(\frac{p_0}{z_0 + h} \right) - 2z_0 \arctan \left(\frac{p_0}{z_0} \right) \right] \\ \tilde{H}_z(p_0, z_0) &= \frac{y}{2} \left[z_0 \ln \left(1 + \frac{p_0^2}{z_0^2} \right) - (z_0 + h) \ln \left(1 + \frac{p_0^2}{(z_0 + h)^2} \right) - 2p_0 \left(\arctan \left(\frac{z_0 + h}{p_0} \right) - \arctan \left(\frac{z_0}{p_0} \right) \right) \right] \end{aligned} \quad (5)$$

The Z-derivatives of functions \tilde{H}_x and \tilde{H}_z in accordance with (5) are given by:

$$\begin{aligned} \frac{d\tilde{H}_x(p_0, z_0)}{dz_0} &= y \left[\arctan \left(\frac{p_0}{h + z_0} \right) - \arctan \left(\frac{p_0}{z_0} \right) \right] \\ \frac{d\tilde{H}_z(p_0, z_0)}{dz_0} &= \frac{y}{2} \left[\ln \left(1 + \frac{p_0^2}{z_0^2} \right) - \ln \left(1 + \frac{p_0^2}{(z_0 + h)^2} \right) \right] \end{aligned} \quad (6)$$

Similarly, the second derivatives of functions \tilde{H}_x and \tilde{H}_z along the Z-axis in accordance with (5) are determined by following expressions:

$$\begin{aligned} \frac{d^2\tilde{H}_x(p_0, z_0)}{dz_0^2} &= y p_0 \left[\frac{1}{z^2 + p_0^2} - \frac{1}{(h + z_0)^2 + p_0^2} \right] \\ \frac{d^2\tilde{H}_z(p_0, z_0)}{dz_0^2} &= y p_0^2 \left[\frac{1}{(z_0 + h)[p_0^2 + (z_0 + h)^2]} - \frac{1}{z_0(z_0^2 + p_0^2)} \right] \end{aligned} \quad (7)$$

Thus, magnetic field H defined by expressions (3) can be written using formulas (5) as follows

$$\begin{aligned} H_x &= \tilde{H}_x(w/2 + x_0, z_0) - \tilde{H}_x(x_0 - w/2, z_0) \\ H_z &= \tilde{H}_z(w/2 + x_0, z_0) - \tilde{H}_z(x_0 - w/2, z_0) \end{aligned} \quad (8)$$

The derivatives of magnetic field H components along the Z-axis, by analogy with (8) and in accordance with (6), are given by:

$$\begin{aligned} \frac{dH_x}{dz_0} &= \frac{d\tilde{H}_x}{dz_0}(w/2 + x_0, z_0) - \frac{d\tilde{H}_x}{dz_0}(x_0 - w/2, z_0) \\ \frac{dH_z}{dz_0} &= \frac{d\tilde{H}_z}{dz_0}(w/2 + x_0, z_0) - \frac{d\tilde{H}_z}{dz_0}(x_0 - w/2, z_0) \end{aligned} \quad (9)$$

The second Z-derivatives of magnetic field H components, by analogy with (8) and in accordance with (7), are given by:

$$\begin{aligned} \frac{d^2 H_x}{dz_0^2} &= \frac{d^2 \tilde{H}_x}{dz_0^2}(w/2 + x_0, z_0) - \frac{d^2 \tilde{H}_x}{dz_0^2}(x_0 - w/2, z_0) \\ \frac{d^2 H_z}{dz_0^2} &= \frac{d^2 \tilde{H}_z}{dz_0^2}(w/2 + x_0, z_0) - \frac{d^2 \tilde{H}_z}{dz_0^2}(x_0 - w/2, z_0) \end{aligned} \quad (10)$$

Using analytical expressions of the magnetic field first and second Z-derivates, one can calculate the interaction force (and its first derivative) between magnet probe and rectangular conductor with current. These calculations for different probe geometry are given in [Appendices](#).

The analysis of interaction between magnet probe and rectangular wire can be performed using a special [Flash application](#). Using this application which is based on the theory of cantilever small oscillations, the probe amplitude, phase and resonance frequency in standart MFM method can be calculated.

Summary

- Derived are analytical expressions for spatial distribution of magnetic field, its first and second derivatives over the surface of rectangular conductor with current (see formulas 8-10).
- Theoretical expressions for spatial distribution of magnetic field, its first and second derivatives as a function of conductor parameters can be analyzed using a special Flash application.

References

1. D.V. Sivukhin. Electricity (General course of physics). Moscow, Nauka 1983. - 688 pp. (in Russian).
2. R. Feinman, R. Leitos, M. Sands. The Feinman lectures on physics. Electricity and magnetism. Moscow, MIR 1977. - 299 pp.

Appendices

Appendix 1. Calculation of the force and force gradient on a cylindrical ferromagnetic probe in the magnetic field of a conductor.

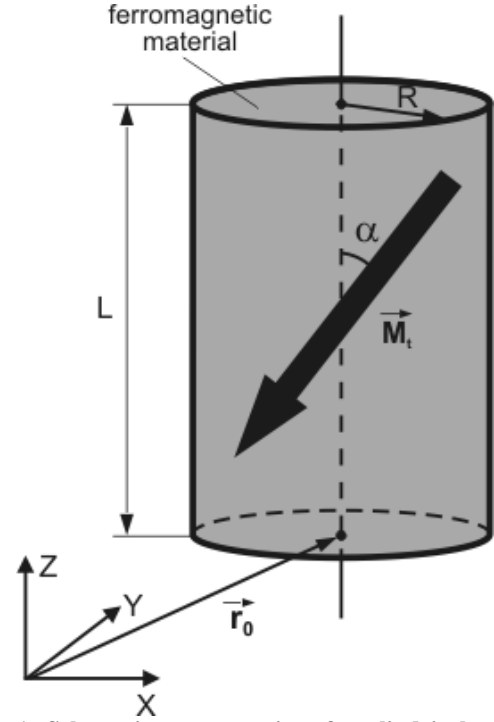


Fig. 1. Schematic representation of a cylindrical probe. Vector r_0 has coordinates (x_0, y_0, z_0)

As shown in chapter 2.7.3 Interaction of the hard magnetic cantilever with the magnetic field of the studied sample (general case), force F acting on magnetic cantilever and its derivative dF/dz_0 can be calculated integrating the force on elementary volume over all the ferromagnetic material. Taking into consideration the tip shape and supposing that magnetic field along the Y-axis is equal to zero, the force and its Z-derivative can be expressed through function $G(x_0, z)$ in accordance with formulas (1, 2) in chapter 2.7.3 Interaction of the hard magnetic cantilever with the magnetic field of the studied sample (general case) as follows:

$$\begin{aligned} G(x_0, z) &= -2M_t \int_{-R}^R \left(\frac{dH_z}{dz_0}(x_0 + x, z) \cos \alpha + \frac{dH_x}{dz_0}(x_0 + x, z) \sin \alpha \right) \sqrt{R^2 - x^2} dx \\ F(x_0, z_0) &= \int_{z_0}^{z_0+L} G(x_0, z) dz \\ \frac{dF(x_0, z_0)}{dz_0} &= G(x_0, z_0 + L) - G(x_0, z_0) \end{aligned} \quad (1)$$

where derivatives of magnetic field H in the analytic form are given by formulas (9,10) in chapter 2.7.9 Magnetic field of rectangular conductor with current.

Appendix 2. Calculation of the force and force gradient on a spherical ferromagnetic tip in the magnetic field of a conductor.

Let us determine the force and derivative of the force acting on a spherical ferromagnetic tip of radius R and magnetization M_t placed in a magnetic field of a current carrying conductor. Let the magnetization vector M_t be directed throughout the tip volume on the angle α to the Z -axis (Fig. 2).

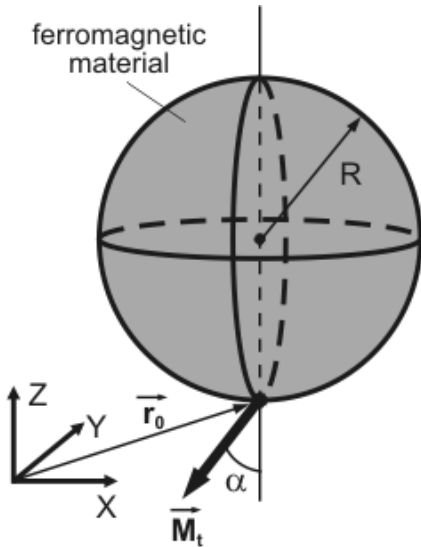


Fig. 2. Schematic representation of a spherical probe.

Vector r_0 has coordinates (x_0, y_0, z_0)

As shown in chapter 2.7.3 Interaction of the hard magnetic cantilever with the magnetic field of the studied sample (general case), force F acting on magnetic cantilever and its derivative dF/dz_0 can be calculated integrating the force on elementary volume over all the ferromagnetic material. Taking into consideration the tip shape and supposing that magnetic field along the Y -axis is equal to zero, the force and its Z -derivative can be expressed in accordance with formulas (1, 2) in chapter 2.7.3 Interaction of the hard magnetic cantilever with the magnetic field of the studied sample (general case) as follows:

$$F(x_0, z_0) = -2M_t \int_0^{2R} \int_{-a(z)}^{a(z)} \left(\frac{dH_z}{dz_0}(x_0 + x, z_0 + z) \cos \alpha + \frac{dH_x}{dz_0}(x_0 + x, z_0 + z) \sin \alpha \right) \sqrt{a(z)^2 - x^2} dx$$

$$\frac{dF(x_0, z_0)}{dz_0} = -2M_t \int_0^{2R} \int_{-a(z)}^{a(z)} \left(\frac{d^2 H_z}{dz_0^2}(x_0 + x, z_0 + z) \cos \alpha + \frac{d^2 H_x}{dz_0^2}(x_0 + x, z_0 + z) \sin \alpha \right) \sqrt{a(z)^2 - x^2} dx$$

(2)

where $a(z) = \sqrt{R^2 - (z - R)^2}$ and derivatives of magnetic field H in analytic form are given by formulas (9,10) in chapter 2.7.9 Magnetic field of rectangular conductor with current.

Appendix 3. Calculation of the force and force gradient on a conical tip covered with a ferromagnetic film in the magnetic field of a conductor.

Let us determine the force and derivative of the force acting on a conical tip covered with a ferromagnetic film placed in a magnetic field of a current-carrying conductor. The tip has radius R , length L and cone angle θ ; the ferromagnetic film has thickness H_{film} and magnetization M_t directed along the Z -axis (Fig. 3).

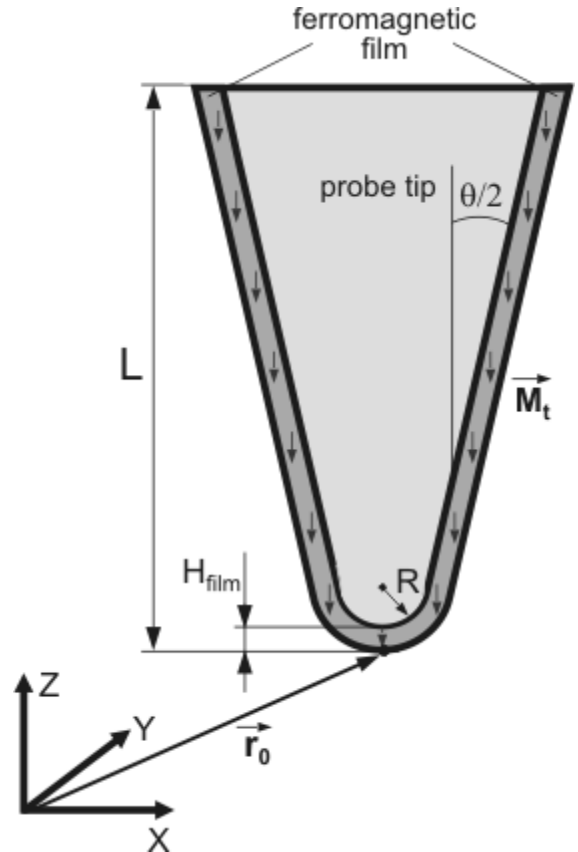


Fig. 3. Section of a conical probe covered with a ferromagnetic film.

Vector r_0 has coordinates (x_0, y_0, z_0)

As shown in chapter 2.7.3 Interaction of the hard magnetic cantilever with the magnetic field of the studied sample (general case), force F acting on magnetic cantilever and its derivative dF/dz_0 can be calculated integrating the force on elementary

volume over all the ferromagnetic material. It shall be convenient to perform the volume integration in three steps.

The first step is the determination of the force and its derivative acting on the spherical part of the tip. Supposing the magnetic field along the Y-axis for this part equals to zero, the force and its Z-derivative can be expressed in accordance with formulas (1, 2) in chapter 2.7.3 Interaction of the hard magnetic cantilever with the magnetic field of the studied sample (general case) as follows:

$$F_1(x_0, z_0) = -2M_t \int_0^{H_{film}} dz \int_{-a(z)}^{a(z)} \frac{dH_z(x_0 + x, z_0 + z)}{dz_0} \sqrt{a(z)^2 - x^2} dx$$

$$\frac{dF_1(x_0, z_0)}{dz_0} = -2M_t \int_0^{H_{film}} dz \int_{-a(z)}^{a(z)} \frac{d^2 H_z(x_0 + x, z_0 + z)}{dz_0^2} \sqrt{a(z)^2 - x^2} dx$$
(3)

where $a(z) = \sqrt{(R + H_{film})^2 - (z - R - H_{film})^2}$ and derivatives of magnetic field H in analytic form are given by formulas (9,10) in chapter 2.7.9 Magnetic field of rectangular conductor with current.

The second step is the determination of the force and its derivative on the nonmagnetic internal cone supposing that the magnetization vector throughout the cone volume is nonzero and coincides with M_t . This operation is also performed in accordance with formulas (1), (2) in chapter 2.7.3 Interaction of the hard magnetic cantilever with the magnetic field of the studied sample (general case) to give:

$$F_2(x_0, z_0) = -2M_t \int_{H_{film}}^L dz \int_{-b(z)}^{b(z)} \frac{dH_z(x_0 + x, z_0 + z)}{dz_0} \sqrt{b(z)^2 - x^2} dx$$

$$\frac{dF_2(x_0, z_0)}{dz_0} = -2M_t \int_{H_{film}}^L dz \int_{-b(z)}^{b(z)} \frac{d^2 H_z(x_0 + x, z_0 + z)}{dz_0^2} \sqrt{b(z)^2 - x^2} dx$$
(4)

where

$$b(z) = \frac{z - H_{film} - R \left(1 - \frac{1}{\cos \varphi}\right)}{\operatorname{tg} \varphi} \quad \text{and} \quad \varphi = \frac{\pi}{2} - \frac{\theta}{2}$$

The third step is the determination of the force and its derivative on the outer part of the cone excluding the tip spherical part supposing that the

magnetization vector throughout the cone volume is nonzero and coincides with M_t . In this case

$$F_3(x_0, z_0) = -2M_t \int_{H_{film}}^L dz \int_{-b(z)-H_{film}}^{b(z)+H_{film}} \frac{dH_z(x_0 + x, z_0 + z)}{dz_0} \sqrt{(b(z) + H_{film})^2 - x^2} dx$$

$$\frac{dF_3(x_0, z_0)}{dz_0} = -2M_t \int_{H_{film}}^L dz \int_{-b(z)-H_{film}}^{b(z)+H_{film}} \frac{d^2 H_z(x_0 + x, z_0 + z)}{dz_0^2} \sqrt{(b(z) + H_{film})^2 - x^2} dx$$
(5)

The total force and its derivative on this tip are then given by:

$$F(x_0, z_0) = F_1(x_0, z_0) - F_2(x_0, z_0) + F_3(x_0, z_0)$$

$$\frac{dF(x_0, z_0)}{dz_0} = \frac{dF_1(x_0, z_0)}{dz_0} - \frac{dF_2(x_0, z_0)}{dz_0} + \frac{dF_3(x_0, z_0)}{dz_0}$$
(6)

Appendix 4. Calculation of the force and force gradient on a conical ferromagnetic probe in the magnetic field of a conductor.

Let us determine the force and derivative of the force acting on a conical tip covered by a ferromagnetic film placed in a magnetic field of a current-carrying conductor. The tip has radius R , length L and cone angle θ ; its magnetization M_t is directed on the angle α to the Z-axis (**Fig. 4**).

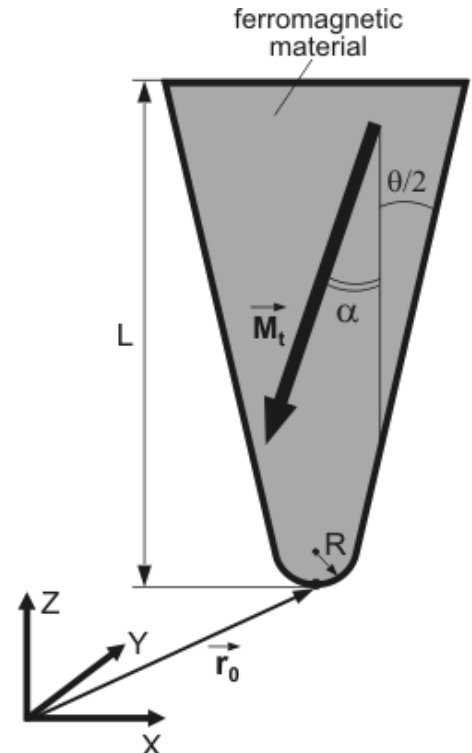


Fig. 4. Section of a conical ferromagnetic probe. Vector r_0 has coordinates (x_0, y_0, z_0)

As shown in chapter 2.7.3 Interaction of the hard magnetic cantilever with the magnetic field of the studied sample (general case), force F acting on magnetic cantilever and its derivative dF/dz_0 can be calculated integrating the force on elementary volume over all the ferromagnetic material. It shall be convenient to perform the volume integration in two steps.

The first step is the determination of the force and its derivative acting on the spherical part of the tip. Supposing the magnetic field along the Y-axis for this part equal to zero, the force and its Z-derivative can be expressed in accordance with formulas (1, 2) in chapter 2.7.3 Interaction of the hard magnetic cantilever with the magnetic field of the studied sample (general case) as follows:

$$\frac{dF_1(x_0, z_0)}{dz_0} = -2M_t \int_0^{H_{film}} dz \int_{-\alpha(z)}^{\alpha(z)} \frac{d^2 H_z(x_0 + x, z_0 + z)}{dz_0^2} \sqrt{\alpha(z) - x^2} dx \quad (7)$$

where $\alpha(z) = \sqrt{R^2 - (z - R)^2}$, $\varphi = \frac{\pi}{2} - \frac{\theta}{2}$ and

derivatives of magnetic field H in analytic form are given by formulas (9,10) in chapter 2.7.9 Magnetic field of rectangular conductor with current.

The second step is the determination of the force and its derivative on the cone excluding its spherical part. This operation is also performed in accordance with formulas (1), (2) in chapter 2.7.3 Interaction of the hard magnetic cantilever with the magnetic field of the studied sample (general case) to give:

$$F_2(x_0, z_0) = -2M_t \int_{R(1-\cos\varphi)}^L dz \int_{-b(z)}^{b(z)} \left(\frac{dH_z}{dz_0}(x_0 + x, z_0 + z) \cos\alpha + \frac{dH_x}{dz_0}(x_0 + x, z_0 + z) \sin\alpha \right) \sqrt{(b(z))^2 - x^2} dx$$

$$\frac{dF_2(x_0, z_0)}{dz_0} = -2M_t \int_{R(1-\cos\varphi)}^L dz \int_{-b(z)}^{b(z)} \left(\frac{d^2 H_z}{dz_0^2}(x_0 + x, z_0 + z) \cos\alpha + \frac{d^2 H_x}{dz_0^2}(x_0 + x, z_0 + z) \sin\alpha \right) \sqrt{(b(z))^2 - x^2} dx \quad (8)$$

where $b(z) = \frac{R(1-1/\cos\varphi)}{\operatorname{tg}\varphi}$.

The total force and its derivative on this tip are then given by:

$$F(x_0, z_0) = F_1(x_0, z_0) + F_2(x_0, z_0)$$

$$\frac{dF(x_0, z_0)}{dz_0} = \frac{dF_1(x_0, z_0)}{dz_0} + \frac{dF_2(x_0, z_0)}{dz_0} \quad (9)$$

2.7.10 Magnetic field of ring with current

Let us calculate the magnetic field generated by direct current J passing through a ring of radius R (Fig. 1). Let the width and thickness of a conductor be much less than R .

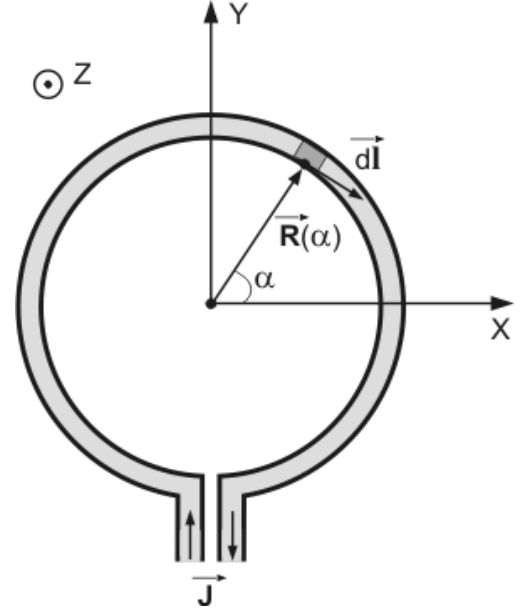


Fig. 1. Schematics of ring with current

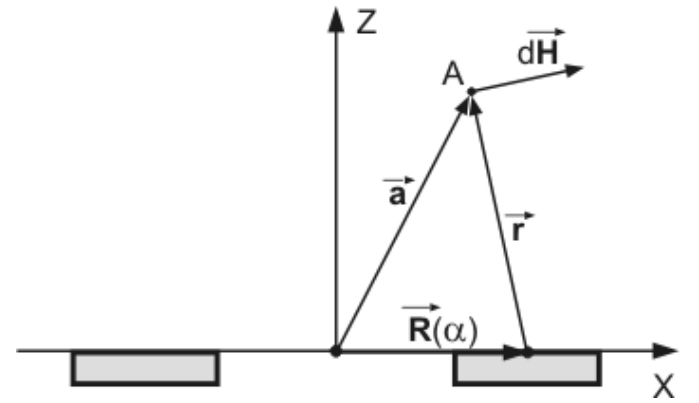


Fig. 2. Cross-section of the ring

According to the Biot-Savart-Laplace law [1, 2], the magnetic field produced by a current-carrying wire element of length dl at distance r from it in Gaussian coordinates is given by

$$dH = \beta \frac{[dl \cdot r]}{r^3} \quad (1)$$

where $\beta = \frac{J}{c}$, c – light velocity

Placing the right-hand coordinate system XYZ into the ring center so that the XY plane lies in the ring plane (Fig. 1, 2) and noting that the problem is

symmetrical relative to the ring center, it is enough to determine the magnetic field distribution in a plane containing vector codirectional with the ring radius and the Z-axis. For mathematical convenience we can choose the plane XZ and determine the magnetic field at point $A(x_0, 0, z_0)$ as shown in **Fig. 2**. The radius-vector r from point A to the ring element dl as a function of angle α is given by the following expression

$$r = a - R(\alpha) = \begin{pmatrix} x_0 - R \cos \alpha \\ y_0 - R \sin \alpha \\ z_0 \end{pmatrix} \quad (2)$$

Elementary vector $d1$ as a function of R and angle α is written as follows:

$$d1 = \begin{pmatrix} R \sin \alpha \\ R \cos \alpha \\ 0 \end{pmatrix} d\alpha \quad (3)$$

Substituting expressions (2) and (3) into formula (1), we get

$$dH(x_0, 0, z_0) = \frac{\beta}{\left(\sqrt{z_0^2 + x_0^2 + R^2 - 2x_0R \cos \alpha}\right)^3} \begin{pmatrix} z_0 R \cos \alpha \\ -z_0 R \sin \alpha \\ R^2 \cos 2\alpha - x_0 R \cos \alpha \end{pmatrix} d\alpha \quad (4)$$

To determine the total magnetic field produced by all the ring at point $A(x_0, 0, z_0)$, one needs to integrate every component of vector dH with respect to α from 0 to 2π . Then, the components X, Y and Z of vector H in accordance with (4) are defined as:

$$\begin{aligned} H_x(x_0, 0, z_0) &= \frac{\beta z_0 R}{\left(\sqrt{z_0^2 + x_0^2 + R^2}\right)^3} \int_0^{2\pi} \frac{\cos \alpha}{(1 - k \cos \alpha)^{3/2}} d\alpha \\ H_y(x_0, 0, z_0) &= 0 \\ H_z(x_0, 0, z_0) &= \frac{\beta R^2}{\left(\sqrt{z_0^2 + x_0^2 + R^2}\right)^3} \left[\int_0^{2\pi} \frac{\cos 2\alpha}{(1 - k \cos \alpha)^{3/2}} d\alpha - \frac{x_0}{R} \int_0^{2\pi} \frac{\cos \alpha}{(1 - k \cos \alpha)^{3/2}} d\alpha \right] \end{aligned} \quad (5)$$

$$\text{where } k = \frac{2x_0R}{z_0^2 + x_0^2 + R^2}.$$

Unfortunately, functions of

$$f(k) = \int_0^{2\pi} \frac{\cos \alpha}{(1 - k \cos \alpha)^{3/2}} d\alpha \quad \text{and}$$

$$g(k) = \int_0^{2\pi} \frac{\cos 2\alpha}{(1 - k \cos \alpha)^{3/2}} d\alpha$$

type can not be expressed through elementary analytic functions, therefore, calculation of H_z and H_x can be performed by numerical integration.

Formulas (5) give the magnetic field distribution in the XZ plane. It is clear that due to the problem symmetry, the magnetic field along the Y-axis is zero and at an arbitrary point $B(x_0, y_0, z_0)$ it is

equal to that at point $A\left(\frac{x_0}{|x_0|} \sqrt{x_0^2 + y_0^2}, 0, z_0\right)$ in the

XZ-plane. Accordingly, formulas (5) are rewritten as:

$$\begin{aligned} H_x(x_0, y_0, z_0) &= \frac{\beta z_0 R}{\left(\sqrt{z_0^2 + x_0^2 + y_0^2 + R^2}\right)^3} \int_0^{2\pi} \frac{\cos \alpha}{(1 - k \cos \alpha)^{3/2}} d\alpha \\ H_z(x_0, y_0, z_0) &= \frac{\beta R^2}{\left(\sqrt{z_0^2 + x_0^2 + y_0^2 + R^2}\right)^3} \left[\int_0^{2\pi} \frac{\cos 2\alpha}{(1 - k \cos \alpha)^{3/2}} d\alpha - \frac{x_0}{|x_0|} \frac{\sqrt{x_0^2 + y_0^2}}{R} \int_0^{2\pi} \frac{\cos \alpha}{(1 - k \cos \alpha)^{3/2}} d\alpha \right] \end{aligned} \quad (6)$$

$$\text{where } k = \frac{x_0}{|x_0|} \frac{2R \sqrt{x_0^2 + y_0^2}}{\left(z_0^2 + x_0^2 + y_0^2 + R^2\right)}.$$

Because z_0 behaves as a parameter in the integrand of functions $f(k)$ and $g(k)$, the first and second Z-derivatives of the magnetic field components can be obtained by direct differentiation of functions H_z , H_x with respect to z_0 and subsequent numerical integration. For example, the first z_0 - derivative of H_x in accordance with (6) is given by:

$$\frac{dH_x(x_0, y_0, z_0)}{dz_0} = d \left[\frac{\beta z_0 R}{(\sqrt{z_0^2 + x_0^2 + y_0^2 + R^2})^3} \right] \int_0^{2\pi} \frac{\cos \alpha}{(1 - k \cos \alpha)^{3/2}} d\alpha + \frac{\beta z_0 R}{(\sqrt{z_0^2 + x_0^2 + y_0^2 + R^2})^3} \left(\int_0^{2\pi} d \left[\frac{\cos \alpha}{(1 - k \cos \alpha)^{3/2}} \right] da \right) \frac{dk(z_0)}{dz_0} \quad (7)$$

The other components of vector H are calculated similarly. In case $x_0 = 0$, $y_0 = 0$ (point A is on the ring axis) formulas (6,7) are transformed as follows

$$\begin{aligned} H_x &= 0 \\ H_z(z_0) &= \beta \frac{2\pi R^2}{(R^2 + z_0^2)^{3/2}} \\ \frac{dH_z(z_0)}{dz_0} &= -\beta \frac{6\pi R^2 z_0}{(R^2 + z_0^2)^{5/2}} \\ \frac{d^2 H_z(z_0)}{dz_0^2} &= \beta \frac{6\pi R^2 [4z_0^2 - R^2]}{(R^2 + z_0^2)^{7/2}} \end{aligned} \quad (8)$$

Using analytical expressions of the magnetic field first and second Z-derivates, one can calculate the interaction force (and its first derivative) between magnet probe and rectangular conductor with current. These calculations for different probe geometry are given in [Appendices](#).

Summary

Derived are formulas (6-8) for the spatial distribution of the magnetic field and its derivatives along the Z-axis over a current ring.

References

1. D.V. Sivukhin. Electricity (General course of physics). Moscow, Nauka 1983. - 688 pp. (in Russian).
2. R. Feinman, R. Leitos, M. Sands The Feinman lectures on physics. Electricity and magnetism. Moscow, MIR 1977. - 299 pp.

Appendices

Appendix 1. Calculation of the force and force gradient on a cylindrical ferromagnetic probe in the magnetic field of a ring with current.

Let us determine the force and derivative of the force acting on cylindrical ferromagnetic tip of radius R , length L and magnetization M_t placed in a magnetic field of a current-carrying conductor. Let magnetization vector M_t be directed throughout the tip volume on the angle α to the cylinder base normal (Fig. 1).

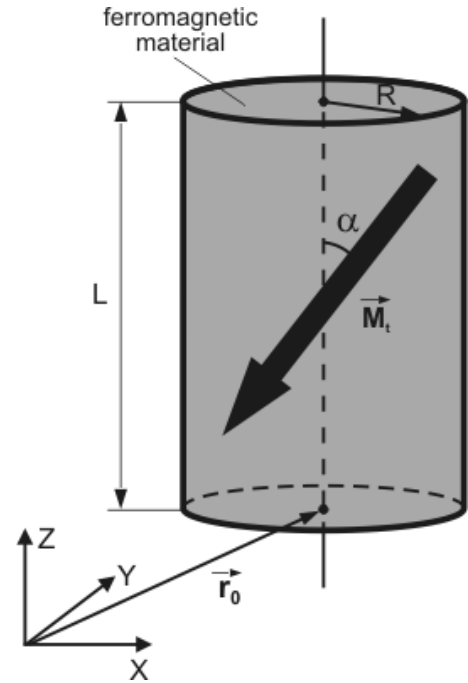


Fig. 1. Schematic representation of a cylindrical probe. Vector r_0 has coordinates (x_0, y_0, z_0) .

As shown in chapter 2.7.3 Interaction of the hard magnetic cantilever with the magnetic field of the studied sample (general case), force F acting on magnetic cantilever and its derivative dF/dz_0 can be calculated integrating the force acting on the elementary volume over all the ferromagnetic material. It shall be convenient to perform the integration of an arbitrary function $f(x, y, z)$ over the cylinder volume in cylindrical coordinates $x = r \cos \varphi$ $y = r \sin \varphi$ $z = z$ which gives

$$\iiint_V f(x, y, z) dx dy dz = \int_0^L \int_0^{2\pi} \int_0^R r f(r \cos \varphi, r \sin \varphi, z) dr d\varphi dz \quad (1)$$

Thus, changing variables $\tilde{x} = x_0 + r \cos \varphi$, $\tilde{y} = y_0 + r \sin \varphi$, $\tilde{z} = z$ we find that the force and its Z-derivative in accordance with formulas (1, 2) in chapter 2.7.3 Interaction of the hard magnetic cantilever with the magnetic field of the studied sample (general case) and (1) are determined through function $G(x_0, y_0, \tilde{z})$ as follows

$$G(x_0, y_0, \tilde{z}) = -M_t \int_0^{2\pi} d\varphi \int_0^R r \left(\frac{dH_z}{dz_0}(\tilde{x}, \tilde{y}, \tilde{z}) \cos \alpha + \frac{dH_x}{dz_0}(\tilde{x}, \tilde{y}, \tilde{z}) \sin \alpha \right) dr$$

$$F(x_0, y_0, z_0) = \int_{z_0}^{z_0+L} G(x_0, y_0, \tilde{z}) d\tilde{z}$$

$$\frac{dF(x_0, y_0, z_0)}{dz_0} = G(x_0, y_0, z_0 + L) - G(x_0, y_0, z_0) \quad (2)$$

where derivatives of magnetic field H in analytic form are given by formulas (6,7) in chapter 2.7.10 Magnetic field of ring with current.

Appendix 2. Calculation of the force and force gradient on a spherical ferromagnetic tip in the magnetic field of a ring with current.

Let us determine the force and derivative of the force acting on spherical ferromagnetic tip of radius R and magnetization M_t placed in a magnetic field of a current ring. Let the magnetization vector M_t be directed on the angle α to the Z-axis (Fig. 2).

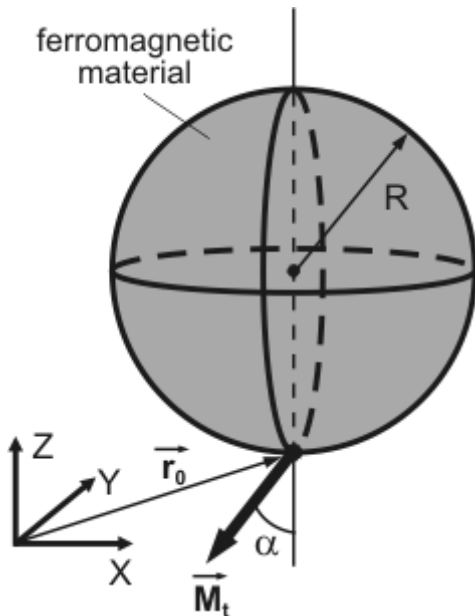


Fig. 2. Schematic representation of a spherical probe. Vector r_0 has coordinates (x_0, y_0, z_0)

As shown in chapter 2.7.3 Interaction of the hard magnetic cantilever with the magnetic field of the studied sample (general case), force F acting on magnetic cantilever and its derivative dF/dz_0 can be calculated integrating the force acting on the elementary volume over all the ferromagnetic material. It shall be convenient to perform the integration of an arbitrary function $f(x, y, z)$ over the sphere volume in spherical coordinates $x = r \sin \vartheta \cos \varphi$, $y = r \sin \vartheta \sin \varphi$, $z = r \cos \vartheta$ which gives

$$\iiint_V f(x, y, z) dx dy dz = \int_{-R}^R \int_0^{2\pi} \int_0^\pi r^2 \sin \vartheta f(r \sin \vartheta \cos \varphi, r \sin \vartheta \sin \varphi, r \cos \vartheta) d\vartheta d\varphi dr \quad (3)$$

Thus, changing variables $\tilde{x} = x_0 + r \sin \vartheta \cos \varphi$, $\tilde{y} = y_0 + r \sin \vartheta \sin \varphi$, $\tilde{z} = z_0 + R + r \cos \vartheta$ we find that the force and its Z-derivative in accordance with formulas (1, 2) in chapter 2.7.3 Interaction of the hard magnetic cantilever with the magnetic field of the studied sample (general case) and (3) are determined as follows

$$F(x_0, y_0, z_0) = -M_t \int_{-R}^R dr \int_0^{2\pi} d\varphi \int_0^\pi r^2 \sin \vartheta \left(\frac{dH_z}{dz_0}(\tilde{x}, \tilde{y}, \tilde{z}) \cos \alpha + \frac{dH_x}{dz_0}(\tilde{x}, \tilde{y}, \tilde{z}) \sin \alpha \right) d\vartheta$$

$$\frac{dF(x_0, y_0, z_0)}{dz_0} = -M_t \int_{-R}^R dr \int_0^{2\pi} d\varphi \int_0^\pi r^2 \sin \vartheta \left(\frac{d^2 H_z}{dz_0^2}(\tilde{x}, \tilde{y}, \tilde{z}) \cos \alpha + \frac{d^2 H_x}{dz_0^2}(\tilde{x}, \tilde{y}, \tilde{z}) \sin \alpha \right) d\vartheta \quad (4)$$

where derivatives of magnetic field H in analytic form are given by formulas (6,7) in chapter 2.7.10 Magnetic field of ring with current.

Appendix 3. Calculation of the force and force gradient on a conical tip covered with a ferromagnetic film in the magnetic field of a current ring.

Let us determine the force and derivative of the force acting on a conical tip covered with a ferromagnetic film placed in a magnetic field of a current-carrying ring. The tip has radius R, length L and cone angle θ ; the ferromagnetic film has thickness H_{film} and magnetization M_t directed along the Z-axis (Fig. 3).

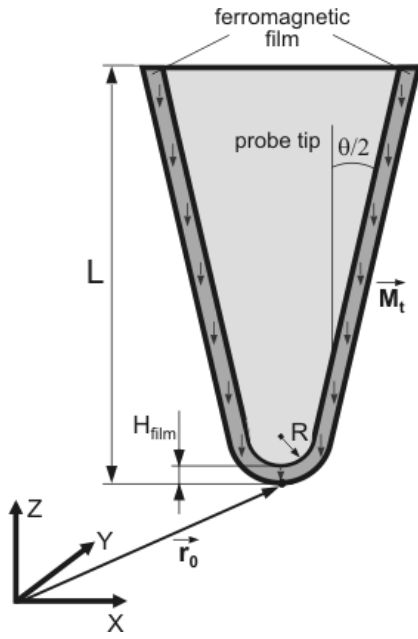


Fig. 3. Section of a conical probe covered with a ferromagnetic film. Vector r_0 has coordinates (x_0, y_0, z_0)

As shown in chapter 2.7.3 Interaction of the hard magnetic cantilever with the magnetic field of the studied sample (general case), force F acting on magnetic cantilever and its derivative dF/dz_0 can be calculated integrating the force acting on the elementary volume over all the ferromagnetic material. It shall be convenient to perform the volume integration in two steps.

The first step is the determination of the force and its derivative acting on the spherical part of the tip. For the sake of mathematical convenience we will perform the integration over the sphere volume in spherical coordinates (see Appendix 2. Calculation of the force and force gradient on a spherical ferromagnetic tip in the magnetic field of a ring with current.).

Thus, changing variables $\tilde{x} = x_0 + r \sin \vartheta \cos \varphi$, $\tilde{y} = y_0 + r \sin \vartheta \sin \varphi$, $\tilde{z} = z_0 + R + H_{film} + r \cos \vartheta$ we find that the force and its Z-derivative on the spherical part of the tip in accordance with formulas (1, 2) in chapter 2.7.3 Interaction of the hard magnetic cantilever with the magnetic field of the studied sample (general case) are determined as follows

$$F_1(x_0, y_0, z_0) = -M_t \int_{-R-H_{film}}^{-R} dr \int_0^{2\pi} d\varphi \int_0^{\pi} r^2 \sin \vartheta \frac{dH_z}{dz_0}(\tilde{x}, \tilde{y}, \tilde{z}) d\vartheta$$

$$\frac{dF_1(x_0, y_0, z_0)}{dz_0} = -M_t \int_{-R-H_{film}}^{-R} dr \int_0^{2\pi} d\varphi \int_0^{\pi} r^2 \sin \vartheta \frac{d^2 H_z}{dz_0^2}(\tilde{x}, \tilde{y}, \tilde{z}) d\vartheta$$

(5)

where derivatives of magnetic field H in analytic form are given by formulas (6,7) in chapter 2.7.10 Magnetic field of ring with current.

The second step is the determination of the force and its derivative acting on the remaining part of ferromagnetic film between two cones. In this case, it is convenient to perform the integration in cylindrical coordinates (see Appendix 1. Calculation of the force and force gradient on a cylindrical ferromagnetic probe in the magnetic field of a ring with current.) with a changing radius of integration that depends on the Z-coordinate. Thus, changing variables $\tilde{x} = x_0 + r \cos \varphi$, $\tilde{y} = y_0 + r \sin \varphi$, $\tilde{z} = z_0 + z$ we find that the force and its Z-derivative acting on the nonspherical part of the tip in accordance with formulas (1, 2) in chapter 2.7.3 Interaction of the hard magnetic cantilever with the magnetic field of the studied sample (general case) are determined as follows

$$F_2(x_0, y_0, z_0) = -2M_t \int_{H_{film}}^L dz \int_0^{2\pi} d\varphi \int_{b(z)}^{b(z)+H_{film}} r \frac{dH_z}{dz_0}(\tilde{x}, \tilde{y}, \tilde{z}) dr$$

$$\frac{dF_2(x_0, y_0, z_0)}{dz_0} = -2M_t \int_{H_{film}}^L dz \int_0^{2\pi} d\varphi \int_{b(z)}^{b(z)+H_{film}} r \frac{d^2 H_z}{dz_0^2}(\tilde{x}, \tilde{y}, \tilde{z}) dr$$

(6)

$$\text{where } b(z) = \frac{z - R(1 - 1/\cos \psi)}{\tan \psi} \text{ и } \psi = \frac{\pi}{2} - \frac{\theta}{2}.$$

The total force and its derivative on this tip are then given by:

$$F(x_0, y_0, z_0) = F_1(x_0, y_0, z_0) + F_2(x_0, y_0, z_0)$$

$$\frac{dF(x_0, y_0, z_0)}{dz_0} = \frac{dF_1(x_0, y_0, z_0)}{dz_0} + \frac{dF_2(x_0, y_0, z_0)}{dz_0}$$

(7)

Appendix 4. Calculation of the force and force gradient on a conical ferromagnetic probe in the magnetic field of a ring with current

Let us determine the force and derivative of the force acting on a conical ferromagnetic tip placed in the magnetic field of a current carrying ring. The tip has radius R , length L and cone angle θ ; its magnetization M_t is directed at angle of α to the Z-axis (Fig. 4).

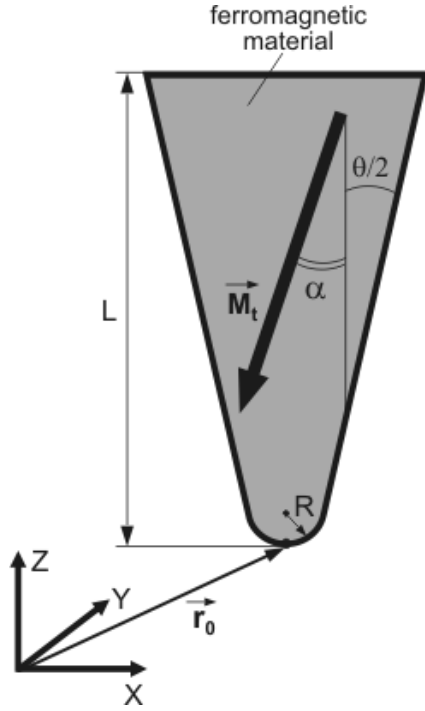


Fig. 4. Section of a conical ferromagnetic probe.
Vector r_0 has coordinates (x_0, y_0, z_0)

As shown in chapter 2.7.3 Interaction of the hard magnetic cantilever with the magnetic field of the studied sample (general case), force F acting on magnetic cantilever and its derivative dF/dz_0 can be calculated integrating the force acting on the elementary volume over all the ferromagnetic material. It shall be convenient to perform the volume integration in two steps.

The first step is the determination of the force and its derivative acting on the spherical part of the tip. It is convenient to perform the integration over the sphere volume in spherical coordinates (see Appendix 2. Calculation of the force and force gradient on a spherical ferromagnetic tip in the magnetic field of a ring with current.). Thus, changing variables $\tilde{x} = x_0 + r \sin \vartheta \cos \varphi$, $\tilde{y} = y_0 + r \sin \vartheta \sin \varphi$, $\tilde{z} = z_0 + R + r \cos \vartheta$, we find that the force and its Z -derivative acting on the spherical part of the tip in accordance with formulas (1, 2) in chapter 2.7.3 Interaction of the hard magnetic cantilever with the magnetic field of the studied sample (general case) are determined as follows

$$F_1(x_0, y_0, z_0) = -M_t \int_{-R}^{-R(1-\cos\psi)} dr \int_0^{2\pi} d\varphi \int_0^\pi r^2 \sin\vartheta \left(\frac{dH_z}{dz_0}(\tilde{x}, \tilde{y}, \tilde{z}) \cos\alpha + \frac{dH_x}{dz_0}(\tilde{x}, \tilde{y}, \tilde{z}) \sin\alpha \right) d\vartheta$$

$$\frac{dF_1(x_0, y_0, z_0)}{dz_0} = -M_t \int_{-R}^{-R(1-\cos\psi)} dr \int_0^{2\pi} d\varphi \int_0^\pi r^2 \sin\vartheta \left(\frac{d^2 H_z}{dz_0^2}(\tilde{x}, \tilde{y}, \tilde{z}) \cos\alpha + \frac{d^2 H_x}{dz_0^2}(\tilde{x}, \tilde{y}, \tilde{z}) \sin\alpha \right) d\vartheta$$

(8)

where $\psi = \frac{\pi}{2} - \frac{\theta}{2}$ and derivatives of magnetic field

H in analytic form are given by formulas (6,7) in chapter 2.7.10 Magnetic field of ring with current.

The second step is the determination of the force and its derivative acting on the cone excluding its spherical part. In this case, it is convenient to perform the integration in cylindrical coordinates (see Appendix 1. Calculation of the force and force gradient on a cylindrical ferromagnetic probe in the magnetic field of a ring with current.) with a changing radius of integration that depends on the Z -coordinate.

Thus, changing variables $\tilde{x} = x_0 + r \cos \varphi$, $\tilde{y} = y_0 + r \sin \varphi$, $\tilde{z} = z_0 + z$ we find that the force and its Z -derivative acting on the conical part of the tip in accordance with formulas (1, 2) in chapter 2.7.3 Interaction of the hard magnetic cantilever with the magnetic field of the studied sample (general case) are determined as follows

$$F_2(x_0, y_0, z_0) = -2M_t \int_{R(1-\cos\psi)}^L dz \int_0^{2\pi} d\varphi \int_0^{b(z)} r \left(\frac{dH_z}{dz_0}(\tilde{x}, \tilde{y}, \tilde{z}) \cos\alpha + \frac{dH_x}{dz_0}(\tilde{x}, \tilde{y}, \tilde{z}) \sin\alpha \right) dr$$

$$\frac{dF_2(x_0, y_0, z_0)}{dz_0} = -2M_t \int_{R(1-\cos\psi)}^L dz \int_0^{2\pi} d\varphi \int_0^{b(z)} r \left(\frac{d^2 H_z}{dz_0^2}(\tilde{x}, \tilde{y}, \tilde{z}) \cos\alpha + \frac{d^2 H_x}{dz_0^2}(\tilde{x}, \tilde{y}, \tilde{z}) \sin\alpha \right) dr$$

(9)

$$\text{where } b(z) = \frac{z - R(1 - 1/\cos\psi)}{\tan\psi}.$$

The total force and its derivative on this tip are then given by:

$$F(x_0, y_0, z_0) = F_1(x_0, y_0, z_0) + F_2(x_0, y_0, z_0)$$

$$\frac{dF(x_0, y_0, z_0)}{dz_0} = \frac{dF_1(x_0, y_0, z_0)}{dz_0} + \frac{dF_2(x_0, y_0, z_0)}{dz_0}$$

(10)

2.7.11 Magnetic field of cylinder domains

Let us calculate the magnetic field generated by a cylindrical domain of radius R and height h along the longitudinal axis of symmetry (Fig. 1). Assume that domain magnetization M is uniform over its volume and is directed along axis Z .

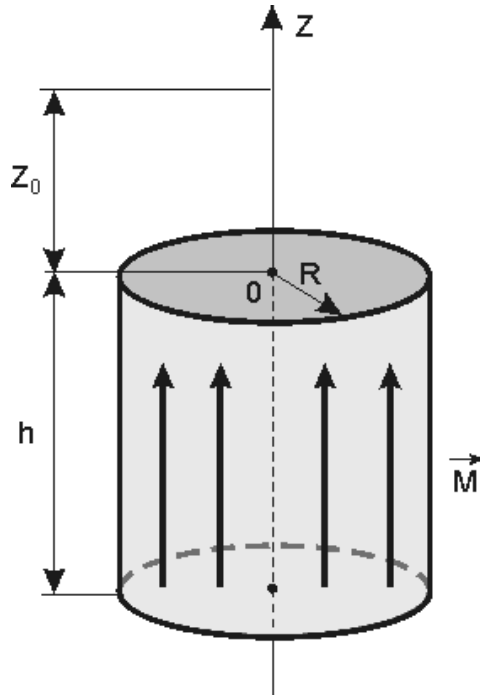


Fig. 1. Schematic representation of a cylindrical domain

Dividing a cylindrical domain into elementary annular domains with magnetic moment $dm = 2\pi Mrdrdz$, where r – distance from domain center to annular domain (ring radius), we can calculate, according to formula (5) in chapter 2.7.1 MFM general concept, the magnetic field created by this elementary domain at distance z :

$$dH = \frac{dm - 3 \cos^2 \theta dm}{(z^2 + r^2)^{3/2}} \quad (1)$$

where $\cos \theta = \frac{r}{\sqrt{z^2 + r^2}}$. It is obvious that due to the cylinder symmetry, the magnetic field of the elementary domain is directed only along the Z -axis. Integrating over the cylinder volume we obtain:

$$H(Z_0) = 2\pi M \int_{Z_0+h}^{Z_0} \int_0^R \left(\frac{1 - 3z^2 / (z^2 + r^2)}{(z^2 + r^2)^{3/2}} \right) r dr dz = 2\pi M \left[\frac{Z_0 + h}{\sqrt{(Z_0 + h)^2 + R^2}} - \frac{Z_0}{\sqrt{Z_0^2 + R^2}} \right] \quad (2)$$

According to formula (2) in chapter 2.7.1 MFM general concept. the signal registered by MFM is determined by the second derivative of the magnetic field. Let us analyze the field and its derivatives dependence on distance Z . The qualitative plot of magnetic field and its first derivative vs. distance Z

in cases $h \gg R$ and $h \ll R$ calculated in accordance with (2) is shown in Fig. 2-5.

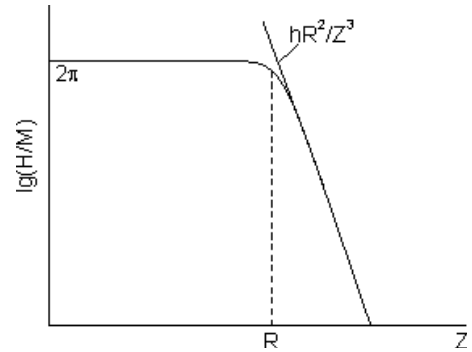


Fig. 2. $H(z)$ plot in case $h \ll R$.
Solid line shows asymptote

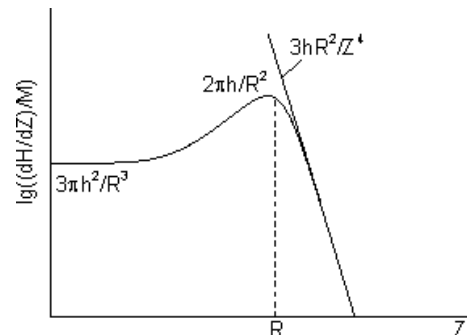


Fig. 3. $dH(z)/dz$ plot in case $h \ll R$.
Solid line shows asymptote.

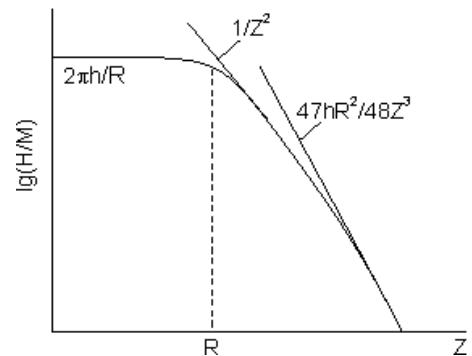


Fig. 4. $H(z)$ plot in case $h \gg R$.
Solid line shows asymptote

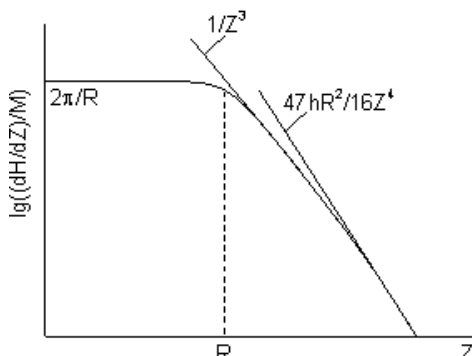


Fig. 5. $dH(z)/dz$ plot in case $h \gg R$.
Solid line shows asymptote

As can be seen from **Fig. 2-5**, the magnetic field decays at distances determined by domain dimensions. Far from domain surface both magnetic field and its derivative have asymptotic behavior. In case $h \ll R$ the second derivative dependence on Z for $Z \gg R$ fits a $1/Z^5$ law. In case $h \gg R$ the second derivative for $Z \geq R$ obeys a $1/Z^4$ law and for $Z \gg R$ – a $1/Z^5$ law.

Thus, if during the qualitative study of magnetic field distribution in the scanning mode a magnetic domain is revealed to be cylindrical, then the analysis of magnetization dependence on distance $F_z(Z) \approx dH/dz$ over the domain center permits to determine magnetic film thickness h and cylinder radius R . The qualitative estimation of ratio h/R can be obtained from the general characteristic of the $F_z(Z)$ dependence.

■ Summary

- Calculated is the magnetic field (2) generated by cylindrical domain of radius R and height h along the longitudinal axis of symmetry.
- If during the qualitative study of magnetic field distribution in the scanning mode it is revealed that magnetic domain is cylindrical, then the analysis of magnetization dependence on distance $F_z(Z) \approx dH/dz$ over domain center permits to determine magnetic film thickness h and cylinder radius R .
- The qualitative estimation of ratio h/R can be obtained from the general characteristic of the $F_z(Z)$ dependence.

2.7.12 Magnetic field of periodic parallel domains

Let us calculate the external magnetic field generated by domains of periodic parallel structure with domains width d_1 and d_2 whose magnetization M is the same in magnitude but reverses orientation from domain to domain (**Fig. 1**).

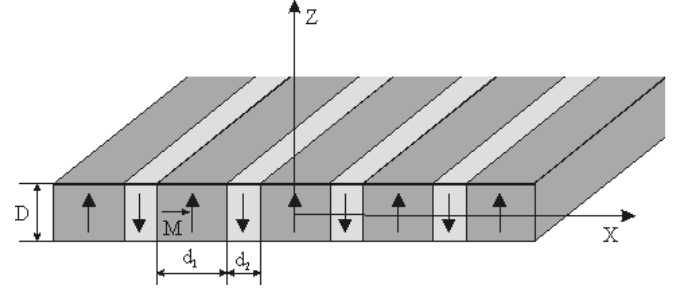


Fig. 1. Schematic representation of magnetic domains periodic parallel structure

We will consider only the case of magnetization vector M orientation perpendicular to a sample surface as shown in **Fig. 1**. We also assume that the magnetic film thickness D is uniform over the sample and its length and width are infinite.

This problem was considered in [] and the results obtained are given here without derivation. The magnetostatic energy of the structure shown in **Fig. 1** is written according to [1] as follows:

$$V_e = \alpha_0 + \sum \alpha_n \sin \frac{n\pi d_1}{d_1 + d_2} \cos \frac{2\pi n x}{d_1 + d_2} \exp\left(-\frac{2\pi n z}{d_1 + d_2}\right) \quad (1)$$

where:

$$\alpha_0 = 2\pi D M \frac{d_1 - d_2}{d_1 + d_2} \quad (2)$$

$$\alpha_n = \exp\left(\frac{\pi n D}{d_1 + d_2}\right) \sinh\left(\frac{\pi n D \sqrt{\mu}}{2(d_1 + d_2)}\right) b_n \quad (3)$$

$$b_n = \frac{8}{\pi} M (d_1 + d_2) \frac{1}{n^2} \left[\sinh \frac{\pi n D \sqrt{\mu}}{d_1 + d_2} + \sqrt{\mu} \cosh \frac{\pi n D \sqrt{\mu}}{d_1 + d_2} \right] \quad (4)$$

$$\mu = 1 + \frac{2\pi M^2}{K} \quad (5)$$

and K – factor of the crystal energy anisotropy. External magnetic field $H(r)$ created by this structure is given by

$$H(r) = -\text{grad}(V_e) \quad (6)$$

Then substituting (1) into (6) we can determine the desired magnetic field at any point in space over the sample.

In MFM, the second derivative of magnetic field with respect to coordinate along a tip vibration direction (see chapter 2.7.1 MFM general concept) is usually measured. Therefore, to qualify the registered in MFM parameters, we have to analyze the qualitative relationship between $\partial^2 H(x, z)/\partial z^2$ and the problem input parameters. Fig. 2-4 show the variation of $\partial^2 H(x, z)/\partial z^2$ along the X-axis calculated according to formulas (1)-(6) at given Z , $D \ll d_2$, $d_2 = d_1/3$ and for various ratios between Z and d_2 .

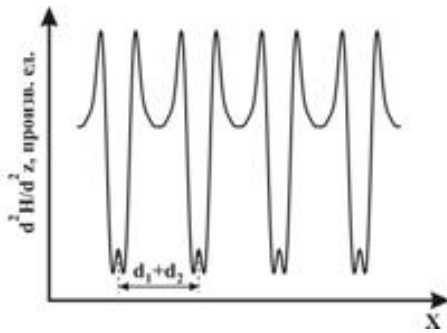


Fig. 2. $\partial^2 H(x, z)/\partial z^2$ qualitative profile along the X-axis at height $Z \ll d_2$.

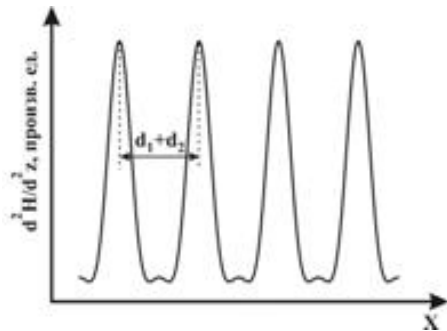


Fig. 3. $\partial^2 H(x, z)/\partial z^2$ qualitative profile along the X-axis at height $Z = d_2$

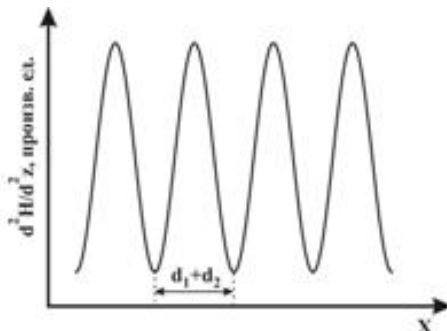


Fig. 4. $\partial^2 H(x, z)/\partial z^2$ qualitative profile along the X-axis at height $Z \gg d_2$

As seen in Fig. 2-4, the studied relations have period equal to $d_1 + d_2$ and are qualitatively different at various values of $D \ll d_1$. The qualitative dependence of $\partial^2 H(x, z)/\partial z^2$ on distance Z at fixed point X (at the border between domains) under condition $D \ll d_1, D \ll d_2$ is shown in Fig. 5.

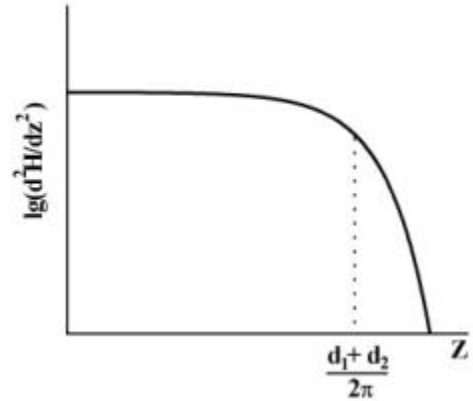


Fig. 5. $\partial^2 H(x, z)/\partial z^2$ qualitative plot along the Z-axis

In this case as in case of a cylindrical domain (see chapter 2.7.11 Magnetic field of cylinder domains), the magnetic field decays at distances determined by the magnetic structure dimensions.

Thus, if during the qualitative study of magnetic field distribution in the scanning mode it is revealed that magnetic domains have laminar structure (Fig. 1), then the comparison of the phase change profiles along the scan line $\varphi(x)$ with results shown in Fig. 2-5 allows to estimate relation between domain sizes and magnetic film thickness. The quantitative analysis is available if the only set of parameters d_1 , d_2 and D is fitted so that calculation according to formulas (1-6) matches best with experimental profiles $\varphi(x)$.

Summary

- Determined is the magnetic field (1)-(6) generated by parallel domains of periodic (laminar) structure having width d_1 and d_2 whose magnetization M is the same in magnitude but reverses orientation from domain to domain.
- If during the qualitative study of magnetic field distribution in the scanning mode it is revealed that magnetic domains have laminar structure, then the comparison of the phase change profiles along the scan line $\varphi(x)$ with results

shown in Fig. 2-5 allows to estimate relation between domain sizes and magnetic film thickness.

- The quantitative analysis is available if the only set of parameters d_1 , d_2 and D is fitted so that calculation according to formulas (1-6) matches best with experimental profiles $\varphi(x)$.

■ References.

1. C. Kooy, U. Enz, Philips Res. Repts. 15, 7-29, (1960)

CONTACT DETAILS

Building 167, Zelenograd, 124460, Moscow, Russia
Tel: +7(095)535-0305, 913-5736
Fax: +7(095) 535-6410, 913-5739

e-mail: spm@ntmdt.ru; <http://www.ntmdt.ru>